Presented at the
International Conference on
Nuclear Physics, Munich, Germany,
August 27 - September 1, 1973

MULTINUCLEON TRANSFER REACTIONS

D. K. Scott

August 1973

Prepared for the U. S. Atomic Energy Commission
under Contract W-7405-ENG-48

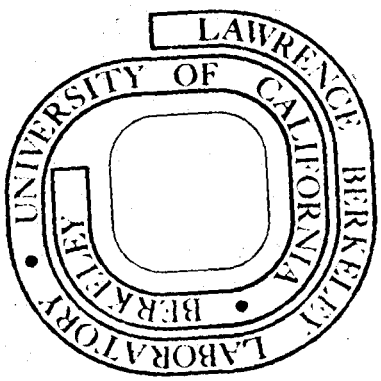

LBL-1991
c.2

DISCLAIMER

(Presented at The International Conference
on Nuclear Physics, Munich, Germany,
August 27 - September 1, 1973)

Multinucleon Transfer Reactions*

D. K. Scott

Nuclear Physics Laboratory
Oxford

and

Lawrence Berkeley Laboratory
University of California
Berkeley, California 94720

* Work performed under the auspices of the U. S. Atomic Energy Commission.

1. Introduction

It is now precisely 21 years since Breit and his collaborators wrote their pioneering paper[1]) entitled "The Possibilities of Heavy-Ion Bombardment in Nuclear Studies", so this year Heavy-Ion Physics has truly come of age. The early years were mainly concerned with incident energies below the Coulomb barrier due partly to the limitations of accelerators but also to the simplicity of the pure Coulomb interaction. Both semi-classical[2]) and DWBA theories[3]) have been developed in this energy region and in some cases have been shown to be equivalent[4]). This region is now sufficiently well understood to permit a recent claim[5]) that "the study of single nucleon transfer reactions with heavy ions below the Coulomb barrier will be used primarily as a means of calibrating in select cases the spectroscopic information obtained from transfer reactions with light ions".

The development of higher energies and better resolution in heavy ion beams from modern Tandems and Cyclotrons, together with improved techniques of particle identification using solid state detectors, magnetic spectrometers and time-of-flight[6]), have led to a resurgence of interest in transfer reactions at energies well above the Coulomb barrier. Over the last few years nuclear physicists have focussed on research with heavy ions, and the view both near and far is one of increasing excitement which has pervaded the conference halls and the research laboratories, dominated the research proposals and preoccupied the funding agencies. This talk is mainly concerned with heavy ion transfer reactions at energies well above the Coulomb barrier, since there lies the promise of the future, in so far as they point towards new aspects of reaction mechnaisms, of nuclear spectroscopy and of correlations in nuclear motion[7]).

2. Direct Reactions with Heavy Ions

The data for the reaction $^{208}Pb(^{16}O,^{15}N)^{209}Bi$ at 104 MeV in Fig. 1 show the characteristics of transfer reactions at high energy[8]). Such reactions have been studied extensively with high resolution at Berkeley using a magnetic spectrometer with combined dE/dX and time-of-flight for particle identification. The reactions selectively populate single particle states of known spectroscopic structure, beyond which there is a continuum often extending over tens of MeV. Typical differential cross sections, measured at Oak Ridge[9]) and Berkeley are shown in Fig. 2. The shapes are largely independent of the transferred angular momentum, since this is small (a few $\hbar$) compared to the angular momentum brought in by the projectile ($\approx$ 100 $\hbar$).

The main features of the data can be understood from simple physical principles[2]). In these reactions $\lambda\!\!\!^{-} \ll R_1 + R_2$, where $\lambda\!\!\!^{-}$ is the wavelength of relative motion ($\approx$ 0.2 fm), and $R_1 + R_2$, the sum of the nuclear radii, is a characteristic length ($\approx$ 13 fm). This localization of the wave-packet leads to the concept of a well-defined classical orbit with a peak in $d\sigma/d\Omega$ at an angle θ_c where the nuclei suffer a grazing collision. For larger angles the nuclei overlap and absorption reduces the transfer cross section, while for smaller angles the nuclei do not come into contact so that the transfer probability is small.

For a Rutherford orbit

$$\operatorname{cosec}\left(\frac{\theta_c}{2}\right) = \frac{2E(R_1 + R_2)}{Z_1 Z_2 e^2} - 1 \qquad (1)$$

where Z_1, Z_2 are the atomic numbers of the colliding nuclei. The position of θ_c as a function of incident energy E is shown on Fig. 2, calculated with a radius parameter of 1.65 fm. Equation 1 predicts that the grazing angle, taken as an average over the initial and final orbits, should move to larger angles with increasing excitation energy (i.e. as E in the final channel decreases). This effect is observed[9]) in Fig. 2(a) for the neutron transfer reaction ($^{12}C, ^{13}C$) and is also predicted by the DWBA calculations shown for the proton transfer reaction ($^{12}C, ^{11}B$) in Fig. 2(b), although in this case the position of the experimental peak is in fact constant[10]). This disagreement, which is greatest for the lowest angular momentum transfer, has been discussed by von Oertzen[11]). If we write the initial and final channel grazing angular momenta,

$$L_i = \eta_i \cot\left(\frac{\theta_c^i}{2}\right) \quad ; \quad L_f = \eta_f \cot\left(\frac{\theta_c^f}{2}\right) \tag{2}$$

where $\eta = Z_1 Z_2 e^2/\hbar v$, the Sommerfeld parameter, then the requirement $L_i \approx L_f$ together with the fact that in proton stripping $\eta_f < \eta_i$ implies $\theta_f < \theta_i$; consequently the absorption and hence the position of the classical maximum are determined primarily by the initial orbit. It is curious that DWBA calculations with standard optical potentials do not reproduce this phenomenon. It illustrates how simple semi-classical theories can be used to give physical insight into more elaborate theories.

The width of the classical maximum ($\delta\theta_c$) has been discussed by Siemens and Becchetti[12]) and by Strutinsky[13]), who show that $\delta\theta_c$ depends on the width of the transfer form factor Δ in orbital angular momentum space. When Δ is

large $\delta\theta_c \propto \Delta$, but when Δ is small, the width is spread by diffraction effects and $\delta\theta_c \propto 1/\Delta$. A simple estimate[14]) gives the minimum width at half maximum,

$$\delta\theta_c \approx \frac{2}{\sqrt{\eta}} \sin\left(\frac{\theta_c}{2}\right) \quad . \tag{3}$$

This esitmate is shown in Fig. 2, and gives the correct trend as a function of energy.

Figure 1(b) illustrates another characteristic feature of heavy ion reactions, viz the apparent j-dependence or enhancement of $j = \ell + 1/2$ states over $j = \ell - 1/2$ states. Such effects can be understood from the selection rules implicit in DWBA theory, and also from simple physical arguments[15]), (this conference 5.130). In a transition from an initial single particle state $j_1\ell_1$ to a final state $j_2\ell_2$, the following selection rules[16]) hold for the angular momentum transfer $\Delta\ell$, in the "no-recoil" approximation (see below)

$$\begin{aligned} |\ell_1 - \ell_2| &\leqslant \Delta\ell \leqslant \ell_1 + \ell_2 \\ |j_1 - j_2| &\leqslant \Delta\ell \leqslant j_1 + j_2 \\ (-1)^{\Delta\ell} &= (-1)^{\ell_1 + \ell_2} \quad . \end{aligned} \tag{4}$$

Applying these rules to the (^{16}O,^{15}N) reaction gives $\Delta\ell = 2$ for the $p_{1/2} \rightarrow p_{3/2}$ transition and $\Delta\ell = 0$ for the $p_{1/2} \rightarrow p_{1/2}$ transition. Since heavy ion reactions favour high angular momentum transfer (typically $\sigma(\Delta\ell = 2)/\sigma(\Delta\ell = 0) \approx 10$) the effect gives rise to an apparent j-dependence. The spectroscopic factors for the $j = \ell - 1/2$ states in this no-recoil DWBA calculation are however in poor agreement with theoretical values, which should be close to unity for all the

states (see Table 1). In order to understand this disagreement, it is necessary to look at the reaction theory in more detail.

The relevant vector diagram for the reaction A(a,b)B with a = b + x and B = A + x is shown[16]) in Fig. 3. For single nucleon transfer the transition probability involves a six dimensional integration over the coordinates $\underline{r}_i$ and $\underline{r}_f$.

$$T^{DWBA} = \int \underline{dr}_f \int \underline{dr}_i \; \chi_f^* (\underline{k}_f, \underline{r}_f) \; \phi_B^* (\underline{r}_2) \; V\phi_a(\underline{r}_1) \; \chi_i(\underline{k}_i, \underline{r}_i) \quad . \qquad (5)$$

The χ's are distorted waves, and the ϕ's represent the relative motions of the nucleon X bound to the cores A or b. In general one must also include spectroscopic factors for the separations A → b + x and B → A + x. In the post interaction form V becomes $V_{bB} - U_{bB}$, the difference between the total interaction in the final channel and the optical potential, and is approximately equal to $V_{bX}(\underline{r}_1)$.

Although the 6D integration has been performed[17,18]), the application to reactions on Pb at over 100 MeV is expensive and it is customary to introduce simplifications to make a separation into two 3D integrals. The most drastic is the "no-recoil" approximation where we set $\underline{r}_f \approx \frac{A}{B} \underline{r}$ and $\underline{r}_i \approx \underline{r}$; here A,B etc. denote masses of the nuclei. Then

$$T_{NR}^{DWBA} = \int \chi_f^* (\underline{k}_f, \tfrac{A}{B} \underline{r}) \; F(\underline{r}) \; \chi_i \; (\underline{k}_i, \underline{r}) \; \underline{dr} \qquad (6)$$

$$F(\underline{r}) = \int \phi_B^* (\underline{r} + \underline{r}') \; V_{bX}(\underline{r}') \; \phi_a(\underline{r}') \; \underline{dr}' \qquad (7)$$

These integrals can be evaluated without further approximation[19,20]. An approximate treatment valid for sub-coulomb energies is also available[21].

The effect of the no-recoil approximation can be estimated[16] by expanding the distorted wave:

$$\chi(\underline{k}, \underline{r} + \underline{\delta r}) = e^{\underline{\delta r} \cdot \underline{\nabla}} \chi(\underline{k},\underline{r}) \approx e^{\underline{\delta r} \cdot \underline{K}(r)} \chi(\underline{k},\underline{r}) \tag{8}$$

where $\underline{K}(\underline{r})$ is the local momentum at point $\underline{r}$. Then eq. (5) reduces to the form of eq. (6) with F replaced by

$$F(\underline{r}) = \int e^{i P(\underline{r}) \cdot \underline{r}'} \phi_B^* (\underline{r} + \underline{r}') V_{bX}(\underline{r}') \phi_a(\underline{r}') \underline{dr}'$$

$$P(\underline{r}) = \frac{X}{B} \underline{K}_f(\underline{r}) + \frac{X}{a} \underline{K}_i(\underline{r}) \quad . \tag{9}$$

The classical picture shows that the main contributions to $F(\underline{r})$ come from distances of the order the sum of the nuclear radii, so that $r' \approx Ra$, the radius of the nucleus. The recoil terms, therefore, introduce additional angular momentum transfers[22] of order P.Ra and also allow unnatural parity terms, through for example the first odd-parity term in the expansion

$$e^{i \underline{R} \cdot \underline{r}'} = 1 + i \underline{R} \cdot \underline{r}' + \cdots \quad . \tag{10}$$

In the (^{16}O,^{15}N) reaction discussed previously, $\Delta\ell = 1$ transfer is allowed in addition to 0, 2. This expansion isthe basis of the approximate inclusion of recoil by Nagarajan[23], and Baltz and Kahana (this conference 5.96). More exact treatments are suggested by Elbaz et al.[24].

The theoretical understanding of heavy ion reactions has also stimulated novel methods of handling the 6D integrals, e.g. Montecarlo techniques[25]), expansion of the distorted waves in a series of plane waves[26]). Tamura and Low[27]) point out the saving in computing time of using interpolation to evaluate the slowly varying form factor from points calculated on a coarser mesh than the rapidly varying distorted waves. Other developements are discussed in this conference (5.97, 5.98 and 5.101).

In semi-classical theories the transition amplitude is calculated by integrating the quantum mechanical matrix element for the transfer along a classical orbit[2,28])

$$T^{SC} = \frac{1}{\hbar} \int \langle \psi_B \, V \, \psi_a \rangle \, dt \tag{11}$$

where the wavefunctions ψ_B, ψ_a refer to particles in moving potentials. In transforming to a stationary frame,

$$\langle \psi_B \, V \, \psi_a \rangle = F(t) \, \exp\left\{ - \frac{i}{\hbar} \, [Q - 1/2 \, X \, \dot{S}^2] \right\}$$

$$F(t) = \int e^{\frac{i}{\hbar} X \dot{S} \cdot \underline{r}'} \, \phi_B(\underline{S}(t) + \underline{r}') \, V(\underline{r}') \, \phi_a(\underline{r}') \, \underline{dr}' \quad . \tag{12}$$

Here Q is the reaction Q-value and $\underline{S}$ is the relative coordinate between the cores. The phase factor involving $X\dot{\underline{S}}$ is obviously closely related (see also eq. 16) to $P(\underline{r})$ in eq. (9) so that F(t) is similar to F(r). The term containing $(Q - 1/2 \, X \, \dot{S}^2)$ replaces the distorted waves. The relationship between the semi-classical and quantal descriptions has also been discussed by Gross[29]).

In Table 1 the spectroscopic factors obtained using some of the above methods[27,28,30]) for the (^{16}O,^{15}N) reaction are compared with the no-recoil calculation. In the semi-classical calculation, the integration in eq. (11) was performed along a Rutherford orbit, ignoring the effects of the nuclear potential, and of absorption[28,31]), which must be included in order to extract absolute values.

The cross sections for heavy-ion transfer reactions are strongly Q-dependent. Buttle and Goldfarb have shown[32]) that the optimum Q-value corresponds to equal distances of closest approach before and after transfer, as expressed by the relation

$$Q_{opt} = \frac{Z_3Z_4 - Z_1Z_2}{Z_1Z_2} E^i_{cM} \quad . \tag{13}$$

The relation gives Q_{opt} = -11 MeV for the ^{208}Pb(^{16}O,^{15}N)^{209}Bi reaction at 104 MeV, but the value is modified due to the effects of angular momentum transfer and absorption processes as discussed by several authors[33-36]). In Fig. 4 the Q-value dependence evaluated using no-recoil DWBA theory[10]) and semi-classical theory[28]) (eqs. 7 and 11) are compared. The two approaches give similar behavior (with $Q_{opt} \approx$ -6 MeV) although there are differences such as a variation of Q_{opt} with angular momentum transfer in the semi-classical theory. This theory can again be used to give insight[37]) into such effects as the double peaking of the $i_{13/2}$ transition.

Although only single nucleon transfers on Pb have been discussed here, detailed studies have also been made on nuclei in the Zr-Mo region[36,38]) in the $f_{7/2}$- shell[36,39,40]), the s-d shell[40]) and in the p-shell[41,42]) using optical model parameters compatible with the elastic scattering data. Equally detailed studies of two nucleon transfers have also been discussed[36,43,44]) recently.

3. Novel Spectroscopic Aspects

The previous section summarized the "state of the art" in nuclear spectroscopy with heavy ions as an extension of light-ion spectroscopy. Heavy ion reactions also open up the possibility of new methods of spectroscopy, e.g. elastic transfer[45]) (this conference, 5.16 - 5.21). In a reaction A(B,A)B, there is coherent interference with elastic scattering A(B,B)A, where the center of mass angles for the two processes are related by $\theta_B = \pi - \theta_A$. The interference gives rise to structure in the angular distributions as illustrated[46]) in Fig. 5 for the reaction $^{29}Si(^{28}Si,^{28}Si)^{29}Si$. The outgoing heavy ions were identified using "time-of-flight", a technique likely to be of increasing importance as accelerators produce ions far beyond the light end of the register currently accessible. The extraction of spectroscopic information for the decomposition $^{29}Si \rightarrow {}^{28}Si + n$ does not depend on obtaining an absolute cross section, but rather on the shape of an interference pattern. Other advantages of heavy ion reactions (this conference, 5.134) occur when a number, P, states are excited in the residual nucleus in conjunction with Q, states in the ejectile giving $P \times Q$ possible combinations with considerably fewer unknown spectroscopic factors; the results must yield self consistency.

4. Diffraction Effects

As discussed in section 2, the differential cross sections for heavy ion transfer reactions are often featureless and devoid of any diffractive structure. In Table 2, some characteristic parameters are shown. For reactions with ^{12}C on ^{208}Pb at 114 MeV, the classical maximum is well defined

($\theta_c >> \delta\theta_c$). The period of diffraction oscillations (π/kR) is small and further, since the ratio of the diffraction cross section to the Rutherford cross section is inversely proportional to η (≈ 25), these reactions are dominated, as we have seen, by the classical distribution. The second example of $^{14}N + ^{48}Ca$ at 50 MeV has been studied at Brookhaven[47]) (this conference 5.132) and the most recent results are shown in Fig. 6. Diffractive effects of the expected period are clearly present in the data which agree in almost every detail with DWBA calculations including recoil effects. The cross sections are also characteristic of the angular momentum transfer at angles forward of 15°. The calculations used an optical potential with V = 70 MeV, W = 10 MeV, a = 0.5 fm and R = 7.4 fm, in which the anomalously weak absorption is essential[48]) in producing sufficient amplitude in orbits from opposite sides of the nucleus to create diffractive oscillations of period π/kR. This group has previously found weak absorption crucial to the understanding[49]) of forward peaking in the differential cross sections for the ($^{18}O, ^{16}O$) on isotopes of Ni. These finer aspects of heavy ion reactions are likely to give greater insight into the heavy ion optical potentials in the future[50]). (See also this conference, 5.133.)

Table 2 shows that reactions with $^{12}C + ^{12}C$ at high energy have η values comparable to light ion reactions, and also that the position of the classical maximum is of the same order as the width. In this case, the classical maximum is no longer defined and quantum mechanical effects should be dominant. Figure 7 shows that no-recoil DWBA theory predicts strong oscillations in the differential cross sections, whereas the data for the reaction $^{13}C(^{12}C, ^{13}C)^{12}C$ at 87 MeV are almost monotonically decreasing.

Devries and Kubo[51]) have shown that the additional angular momentum transfer permitted in the calculations including recoil (discussed in section 2) give rise to oscillations which are out of phase and the resultant is in satisfactory agreement with the data. Such featureless differential cross sections are characteristic of a wide variety of 1 and 2 nucleon transfer reactions in the pioneering work of the Yale group[52]) on high energy reactions with heavy ions, which were difficult to interpret using the diffraction models of Frahn and Venter[53]) and of Dar[54]). Devries has also illustrated[55]) cases where a larger number of allowed angular momentum transfers give rise to pronounced oscillations, e.g. $^{11}B(^{12}C,^{11}B)^{12}C$ where $\Delta\ell = 0$, 1 and 2 are allowed.

5. Simple Configurations in Light Nuclei

The featureless differential cross sections discussed in the last section suggest that many high energy reactions with heavy ions are unpromising as probes of nuclear structure. The high angular momenta associated with recoil effects can however be exploited, to perform selective spectroscopy on light nuclei. For the reaction A(a,b)B with a = b + x and B = A + x, we write the recoil momentum as in eq. (9), using k_i, k_f in place of the local momenta K_i, K_f, and X, A etc. to denote nuclear masses

$$P \approx \frac{x}{A + x} \underline{k}_f + \frac{x}{b + x} \underline{k}_i \tag{14}$$

or in terms of velocities, since

$$\underline{k}_f = \frac{(A + x)\, b}{(A + x + b)} \frac{\underline{v}_f}{\hbar}, \qquad k_i = \frac{(b + x)\, A}{(A + x + b)} \frac{\underline{v}_i}{\hbar} \tag{15}$$

$$P \approx \frac{x(A\underline{v}_i + b\underline{v}_f)}{\hbar(A + x + b)} \approx \frac{x\bar{v}}{\hbar} \qquad (16)$$

where $\bar{v}$ is an average of the initial and final velocities. The associated angular momentum transfer of $\underline{P} \circ \underline{R}_T$, where R_T is the radius of the target, is equal approximately to the angular momentum carried by the transferred mass at the surface of the target nucleus. At small angles, this is the dominant means of transferring angular momentum, and for single nucleon transfer with projectiles of energy 10 MeV/nucleon has a value 2 $\hbar$ for p-shell targets and 3 $\hbar$ for fp-shell targets, i.e. it is closely matched to the single particle orbitals, available outside closed shells. This principle can be extended to the transfer of several nucleons, and, combined with the apparent preference for heavy ion reactions to transfer spatially localized clusters, leads to the identification of high spin states in light nuclei which are of current interest to the theory of nuclear models[56]. (See also invited talks by Arima and McGrory, this conference.)

Similar studies have been initiated at Texas A and M[57]. Figure 8 shows a spectrum for three nucleon transfer ($^{10}B, ^{7}Li$) and ($^{10}B, ^{7}Be$) on ^{12}C at 100 MeV. The states at 12.89 and 15.36 MeV in ^{15}O have been interpreted by the Oxford Group as three nucleon cluster states of spin $11/2^-$ and $13/2^+$. Table 3 gives a comparison between the experimental and theoretical cross sections for the reaction $^{12}C(^{12}C, ^{9}Be)^{15}O$ (which show features almost identical to the example in Fig. 8), using semi-classical theory[33]) to describe the reaction dynamics and cluster spectroscopic amplitudes (see e.g. this conference 3.49). The results strongly suggest identification of the $9/2^+$ predicted at

9.08 MeV and $7/2^+$ at 10.8 MeV with the observed excitations at 9.64 and 10.47 MeV. No DWBA calculations have been performed on these data, which must of necessity treat recoil effects exactly, but it is clearly a fertile field for future spectroscopic investigations[58].

Another interesting aspect of these reactions is the energy dependence for which the semi-classical predictions[33,37] are shown in Fig. 9. Due to the increasing effects of recoil at higher energies, high spin states are enhanced, in approximate agreement with the experimental data of Fig. 10. These excitation functions could possibly be used as a means of inferring the J-values of high spin states. So far there have been few experimental techniques available, although some interesting developments are reported at this conference (e.g. 5.81).

6. Multistep Processes

Most heavy ion transfer data suggest that reactions proceed in a direct fashion, transferring a cluster between nuclear cores which are otherwise left undisturbed. Second order processes of the type illustrated in Fig. 11 were, however, expected to play an even more important role than they are now known to do in light ion reactions[59]. Recently, some of the implications for heavy ion reactions have been investigated[60-63].

Figure 12 shows results[60] for the two nucleon transfer reaction $^{40}Ca(^{18}O,^{20}Ne)^{38}Ar$. The differential cross sections for transitions with the ejectile excited are forward peaked compared to the usual classical distributions predicted by the DWBA. As shown at the bottom of the figure, Tamura and Low suggest that the effect could arise from higher order processes

for which the projectile in a deformed excited state makes a closer collision with the nucleus, and the attractive nuclear force causes forward focussing. This interpretation is supported to some extent by preliminary coupled channels calculations shown on the right. It remains, however, to check the coupled channels Born approximation (CCBA) with inclusion of recoil effects, since as mentioned previously, forward peaked cross sections can also be explained by weak absorption[49]. Further data on these processes appear in this conference (5.131).

Another interesting development is discussed by Glendenning and Ascuitto[62] (this conference, 5.155), who show that interference between direct and indirect routes for the $^{120}Sn(^{18}O,^{16}O)^{122}Sn$ reaction leads to a flattening of the angular distribution for excitation of the 2^+ state (see Fig. 13). Some preliminary data from Oxford (this conference 5.156) suggest that this effect may be less strong; however, there are critical parameters in the calculation, such as the optical potentials and the nuclear deformation β for which the value was taken from light ion inelastic scattering. A further prediction is that the interference should be of opposite sign in the $^{122}Sn(^{16}O,^{18}O)^{120}Sn$ reaction. These studies may prove to be a sensitive method of studying nuclear deformations in the future.

7. Nuclear Correlations

A classic example of correlated nucleon transfer in light ion reactions appeared in the (t,p) reaction on Sn isotopes[64], where there is an enhancement of approximately 30 in the two neutron transfer to the superfluid pairing vibrational states over sequential neutron transfer. Since we have shown that

heavy ion reactions favour correlated cluster transfer, it is surprising that 2n transfer reactions have not shown this enhancement[65]. However, the data for the reaction $^{120}Sn(^{18}O,^{16}O)^{122}Sn$ discussed in the last section (Fig. 13) showed that the superfluid ground state (0^+) is excited more strongly than the collective vibrational (2^+) state by a factor of 10, although the heavy ion transfer probability favours the larger angular momentum transfer by a factor of 8. The experimental cross section for the 0^+ state was within a factor of 2 of the theoretical value[62], calculated with a BCS superfluid wavefunction for the 0^+ vibration. The transfer of several nucleons could also take place via a sequential process, and within the semi-classical framework, the cross section is given as a product of the individual nucleon[66] transition probabilities, P_1, P_2, $\cdots$,

$$\sigma \approx P_1 P_2 \cdots \times (\text{E.F.}) \times \sigma_{el}$$

where E.F. is the enhancement factor and σ_{el} is the cross section for elastic scattering. From the measured single nucleon cross sections E.F. was deduced to be ≈ 50.

Heavy ion reactions also permit the study of 2p correlations. Some data for the $(^{16}O,^{14}C)$ reaction on several nuclei from Heidelberg[66] are shown in Fig. 14. The transition probability is plotted against a parameter (d_0) to remove nuclear size and kinematic effects. The transfer probability for nuclei with open proton shells, corresponding to the open neutron shells in Sn, (viz. ^{140}Ce, ^{142}Nd and ^{144}Sn) shows enhancement of approximately 30 over nuclei in the Fe, Ni region.

Some recent calculations[67]) on $^{118}Sn(^{120}Sn,^{118}Sn)^{120}Sn$ at 500 MeV show that 90% of the cross section may come from sequential transfer. Similar conclusions were reached by the Brookhaven group in a study of 2n transfers on isotopes of Molybdenum[68]). This subject is likely to be an interesting area of investigation for accelerators of the future. It is also a field where semi-classical theories can be used to provide physical insight.

Since 2p and 2n transfers exhibit correlations, we might also look for four nucleon correlations. Historically, these were investigated first, in particular by the $(^{16}O,^{12}C)$ reaction at Saclay[69]) and were partly responsible for the revival of interest in heavy ion reactions. Data taken with a high resolution spectrometer[70]) for the $^{90}Zr(^{16}O,^{12}C)^{94}Mo$ reaction are shown in Fig. 15. Only a few states are excited in a region of high level density. The quartet model[71]) emphasizes the importance of four-nucleon correlations, the constituent two nucleon pairs having the greatest interaction when they are aligned or anti-aligned. Microscopic form factors were calculated in an aligned quartet scheme[72]) which reduces the huge four nucleon configuration space. The theoretical spectrum shown at the top of the figure was obtained by incorporating this form factor in the generator coordinate formulation of the DWBA[73]). It now seems clear that in addition to the two-nucleon correlations, we can isolate another correlation responsible for the quartet interaction.

In light nuclei, four nucleon correlations are well known[74]) and are discussed in the talk by Arima. It is not possible here to cover the many investigations using Li and He induced reactions[75]). However, the subject is likely to receive new impetus from heavy-ion induced reactions (see e.g. ref. [76])) and in particular from the recently developed techniques for ^{8}Be detection[77]).

Some results for the (α,^{8}Be) reaction[78]), which has been referred to by Kurath as "the (p,d) of α-transfer", are shown in Fig. 16. The $3/2^-$ g.s. and the $7/2^-$, 4.63 MeV state are strongly excited as predicted in the recent tabulation of α-spectroscopic amplitudes by Kurath[79]). The experimental method shows the scope for ingenuity which has been characteristic of the study of heavy-ion reactions. The α's from the ^{8}Be decay were allowed to pass through a divided collimator on either side of a central post, and after traversing a ΔE-detector stopped in a position sensitive detector (see Fig. 17). The two α's generate a position signal corresponding to the region of the post. When the particle identification spectrum is gated by position signals from this region, particle stable nuclei are eliminated and almost complete separation of ^{8}Be events is achieved. Since the position signal also establishes the direction of ^{8}Be, good energy resolution is possible with a large solid angle.

These heavy-ion transfer reactions compliment and extend the information on nuclear correlations accessible through conventional light ion induced reactions. However, there is also the possibility of studying new types of nuclear states, e.g. quasi-molecular states in transfer reaction with heavy-ions[80]).

8. Multinucleon Transfers

Multinucleon transfer reactions are the subject of ardent research at the present time[81]) in the hope that they will selectively excite multiparticle-multihole states. A well documented example is the ^{12}C(^{12}C,α)^{20}Ne reaction[82]) shown in Fig. 18, where the marked difference in strength of adjacent 2^+ states at 7.833 and 7.421 MeV indicates a strong direct component, since in any statistical process the energy averaged cross section depends only on J^π for

levels at comparable excitation. The excitation function for the 7.83 MeV level, shown on the right, although fluctuating, is superimposed on a large, presumably direct, background. Further evidence is presented in this conference (5.214) that the reaction is 80% direct. However, this reaction is rather special in the sense that the spectroscopic factor for extracting 8 nucleons from ^{12}C is simply related to the α-spectroscopic factor, which is known to be large.

Other eight nucleon transfer reactions have been claimed as direct, e.g. ($^{14}N, ^{6}Li$), partly on the asuumption that the compound nuclear probability for ^{6}Li emission should be small[83]). Complete angular distributions for the $^{12}C(^{14}N, ^{6}Li)^{20}Ne$ reaction were measured at Oxford[84]). They were found to exhibit approximate symmetry around 90° for all states, and could be fitted by a $1/\sin\theta$ distribution expected from the decay of a high spin compound nuclear state. (See Fig. 19.) In addition to the shape, however, the relative and absolute magnitdues contain information on the reaction mechanism. The solid curves in the figure are the results of Hauser-Feshbach calculations by the Yale Group[85]) (this conference, 5.218). The calculations used optical model transmission coefficients from elastic scattering data and a Fermi Gas model for the level densities. The agreement with experiment is excellent.

It appears that although these reactions may not be dominated by the direct transfer characteristic of one, two, three and four nucleon transfer (see this conference, 5.207, 5.147), they may contain other valuable clues to nuclear structure information. For example, an important parameter in the Yale calculation in the Yrast, or maximum angular momentum available in the compound nucleus, which in turn depends on the moment-of-inertia assumed for the compound nucleus.

9. The Future

The changing perspectives between few nucleon and multinucleon transfer reactions discussed in the last section begin to link macroscopic and microscopic properties of nuclei. Liquid drop calculations[86]) indicate the maximum angular momentum at which a nucleus becomes unstable against fission ($\approx 80\ \hbar$ at mass 200). (See this conference, 5.229, 5.230). For reactions where this angular momentum becomes comparable to the grazing angular momentum, one can expect even one and two nucleon transfer reactions to show features very different from those outlined at the beginning of this talk, since then the limiting angular momenta will correspond to internuclear distances where the nuclei overlap strongly.

Some of these features may already be present in the heavy ion experiments conducted at Dubna and Orsay over the last few years[87,88]). (See also this conference, 5.164 - 167). The contour plot of $d^2\sigma/d\Omega\, dQ$ by Siemens[89]) for single proton transfer $^{40}Ar + {}^{232}Th$ at 380 MeV in Fig. 20, shows that the reaction separates into two regions - the quasi-elastic region concentrated at low excitation energies and angles close to a grazing collision, and an inelastic region concentrated at high excitation and forward angles. For multinucleon transfer reactions the quasi-elastic region tends to disappear, and the "coastline" at high excitation is dominant. There exist several interpretations of this "coastline" e.g. direct transitions to a high density of states[90]) (see also this conference, 5.169) or sequential decay of highly excited fragments formed in the initial direct transfers[91]) (see also this conference, 5.238). It has also been attributed to a partial statistical equilibrium in the "neck" between the colliding nuclei[92,93]). The detailed

exploration of these contours will be one of the tasks of the new heavy ion accelerators - accelerating ions far beyond the light end of the heavy-ion register currently accessible - under construction in many countries. In this talk I hope I have been able to give some indication of the influence of Heavy Ion Transfer Reactions on nuclear spectroscopy, on new correlations in nuclear motion and of the challenge to our conventional reaction theories such as the DWBA, diffraction models and semi-classical theories.

Acknowledgments

I wish to thank my colleagues at Oxford and Berkeley for many discussions and ideas. Also, I am grateful to the many research groups who freely contributed unpublished data and interpretations. I should especially like to thank B. G. Harvey for his hospitality at the 88-inch Cyclotron Laboratory, while this talk was prepared.

References

1. G. Breit, M. H. Hull, and R. L. Gluckstern, Phys. Rev. 87, 74 (1952).
2. R. A. Broglia and A. Winther, Physics Report 4, 153 (1972), and references therein.
3. P. J. A. Buttle and L. J. B. Goldfarb, Nucl. Phys. A176, 299 (1971), and references therein.
4. D. Trautmann and K. Alder, Helv. Phys. Acta 43, 363 (1970).
5. K. G. Nair, J. S. Blair, W. Reisdorf, W. R. Wharton, W. J. Braithwaite, and M. K. Mehta, to be published.
6. Some of the recent experimental advances are described by W. von Oertzen in Minerva Symposium on Physics, (Rehovoth, 1973).
7. A review of the literature up to 1967 is given by D. A. Bromley in Lectures at Enrico Fermi Summer School on Nuclear Structure, (Varenna, 1967). A more recent review is given by W. von Oertzen, Nuclear Spectroscopy, ed. by J. Cerny (Academic Press, New York) to be published. Many reviews of recent work are contained in conference proceedings: Nuclear Reactions Induced by Heavy Ions, ed. by R. Bock and W. R. Hering (North-Holland, Amsterdam, 1970); Symposium on Heavy Ion Reactions and Many Particle Excitations (Saclay, 1971), J. Phys. 32, C6 (1971); European Conference on Nuclear Physics (Aix-en-Provence, 1972), J. Phys. 33, C5 (1972); ORNL Heavy Ion Summer Study (Oak Ridge, 1972); Symposium on Heavy Ion Transfer Reactions (Argonne, March 1973).
8. D. G. Kovar, B. G. Harvey, F. G. Pühlhofer, J. Mahoney, D. W. Miller, and M. S. Zisman, Phys. Rev. Letters 29, 1023 (1972).
9. J. S. Larsen, J. L. C. Ford, R. M. Gaedke, K. S. Toth, J. B. Ball, and R. L. Hahn, Phys. Letters 42B, 205 (1972).

10. D. G. Kovar, Symposium on Heavy Ion Transfer Reactions (Argonne, 1973), p. 59.

11. W. von Oertzen, Symposium on Heavy Ion Transfer Reactions (Argonne, 1973), p. 675.

12. P. J. Siemens and F. D. Becchetti, Phys. Letters 42B, 389 (1972).

13. V. M. Strutinsky, Phys. Letters 44B, 245 (1973).

14. D. M. Brink, private communication.

15. F. Pougheon and P. Roussel, Phys. Rev. Letters 30, 1223 (1973).

16. G. R. Satchler, Symposium on Heavy Ion Transfer Reactions (Argonne, 1973), p. 145, and references therein.

17. R. M. Devries and K. I. Kubo, Phys. Rev. Letters 30, 325 (1973).

18. R. Bock and H. Yoshida, Nucl. Phys. A189, 177 (1972).

19. T. Sawaguri and W. Tobocman, J. Math. Phys. 8, 2223 (1967).

20. F. Schmittroth, W. Tobocman, and A. A. Golastaneh, Phys. Rev. C1, 377 (1970).

21. P. J. A. Buttle and L. J. B. Goldfarb, Nucl. Phys. 78, 409 (1966).

22. L. R. Dodd and K. R. Greider, Phys. Rev. Letters 14, 959 (1965).

23. M. A. Nagarajan, Nucl. Phys. A196, 32 (1972); Nucl. Phys. A209, 485 (1973).

24. E. Elbaz, J. Meyer, and R. S. Nahabetian, Nucl. Phys. A205, 299 (1973).

25. B. F. Bayman and D. H. Feng, Nucl. Phys. A205, 513 (1973).

26. L. A. Charlton, Phys. Rev. Letters 31, 116 (1973); Symposium on Heavy Ion Transfer Reactions (Argonne, 1973), p. 161.

27. T. Tamura and K. S. Low, to be published.

28. D. M. Brink, P. N. Hudson, and M. Pixton, to be published.

29. D. H. E. Gross, Phys. Letters 43B, 371 (1973).

30. D. G. Kovar, B. G. Harvey, F. D. Becchetti, J. Mahoney, D. L. Hendrie, H. Homeyer, W. von Oertzen, and M. A. Nagarajan, Phys. Rev. Letters 30, 1075 (1973).

31. R. A. Broglia, S. Landowne, and A. Winther, Phys. Letters 40B, 293 (1972).

32. P. J. A. Buttle and L. J. B. Goldfarb, Nucl. Phys. A115, 461 (1968).

33. D. M. Brink, Phys. Letters 40B, 37 (1972).

34. J. P. Schiffer, H. J. Körner, R. H. Siemssen, K. W. Jones, and A. Schwarzschild, Phys. Letters 44B, 47 (1973).

35. M. Kleber and R. Beck, Phys. Letters 43B, 98 (1973).

36. P. R. Christensen, V. I. Manko, F. D. Becchetti, and R. J. Nickles, Nucl. Phys. A207, 33 (1973).

37. N. Anyas-Weiss, J. Becker, T. A. Belote, J. C. Cornell, P. S. Fisher, P. N. Hudson, A. Menchaca-Rocha, A. D. Panagiotou, and D. K. Scott, Phys. Letters 45B, 231 (1973).

38. M. S. Zisman, F. D. Becchetti, B. G. Harvey, D. G. Kovar, J. Mahoney, and J. D. Sherman, Lawrence Berkeley Laboratory Report LBL-1676, to be published.

39. H. J. Körner, G. C. Morrison, L. R. Greenwood, and R. H. Siemssen, Phys. Rev. C7, 107 (1973).

40. J. V. Maher, K. A. Erb, and R. W. Miller, Phys. Rev. C7, 651 (1973).

41. U. C. Schlotthauer-Voos, H. G. Bohlen, W. von Oertzen, and R. Bock, Nucl. Phys. A180, 385 (1972).

42. U. C. Schlotthauer-Voos, R. Bock, H. G. Bohlen, H. H. Guthrod, and W. von Oertzen, Nucl. Phys. A186, 225 (1972).

43. R. A. Broglia, R. Liotta, A. Winther, B. Nilsson, and T. Kammuri, to be published.

44. F. D. Becchetti, D. G. Kovar, B. G. Harvey, D. L. Hendrie, H. Homeyer, J. Mahoney, W. von Oertzen, and N. K. Glendenning, to be published, and references therein.

45. W. von Oertzen, Nucl. Phys. A148, 529 (1970); A. Gamp et al., Z. fur Physik (in press); C. Alex McMahan and W. Tobocman, Nucl. Phys. A202, 561 (1973).

46. K. D. Hildenbrand, R. Bock, H. G. Bohlen, P. Braun-Munzinger, D. Fick, C. K. Gelbke, W. von Oertzen, and W. Weiss, Phys. Letters 42B, 425 (1972)

47. M. J. Schneider, C. Chasman, E. H. Auerbach, A. J. Baltz, and S. Kahana, Phys. Rev. Letters 31, 320 (1973).

48. C. Chasman, S. Kahana, and M. Schneider, to be published.

49. E. H. Auerbach, A. J. Baltz, P. D. Bond, C. Chasman, J. D. Garrett, K. W. Jones, S. Kahana, M. J. Levine, M. Schneider, A. Z. Schwarzschild, and C. E. Thorn, Phys. Rev. Letters 30, 1078 (1973).

50. P. R. Christensen, O. Hansen, J. S. Larsen, D. Sinclair, and F. Videbaek, Phys. Letters 45B, 107 (1973).

51. R. M. Devries, and K. I. Kubo, Phys. Rev. Letters 30, 325 (1973).

52. J. Birnbaum, J. C. Overley, and D. A. Bromley, Phys. Rev. 157, 787 (1967).

53. W. E. Frahn and R. H. Venter, Nucl. Phys. 59, 651 (1964).

54. A. Dar, Phys. Rev. 139, B1193 (1965).

55. R. M. Devries, Symposium on Heavy Ion Transfer Reactions (Argonne, 1973), p. 189.

56. D. K. Scott, P. N. Hudson, P. S. Fisher, N. Anyas-Weiss, C. U. Cardinal, A. D. Panagiotou, P. J. Ellis, and B. Buck, Phys. Rev. Letters 28, 1659 (1972).

57. K. Nagatani, D. H. Youngblood, R. Kenefick, and J. Bronson, Phys. Rev. Letters 31, 250 (1973).

58. A detailed account by N. Anyas-Weiss et al. is to be published in Physics Reports.

59. R. J. Ascuitto and N. K. Glendenning, Phys. Rev. C2, 1260 (1970).

60. K. S. Low and T. Tamura, Symposium on Heavy Ion Transfer Reactions (Argonne, 1973), p. 655.

61. W. Tobocman, R. Ryan, A. J. Baltz, and S. Kahana, Nucl. Phys. A205, 193 (1973).

62. N. K. Glendenning and R. J. Ascuitto, Phys. Letters 45B, 85 (1973).

63. S. Landowne, R. A. Broglia, and R. Liotta, Phys. Letters 43B, 160 (1973).

64. R. A. Broglia, O. Hansen, and C. Riedel, to be published.

65. R. H. Siemssen, Proceedings of the Symposium on Two Nucleon Transfer and Pairing Excitations (Argonne, 1972), p. 273.

66. W. von Oertzen, H. G. Bohlen, and B. Gebauer, Nucl. Phys. A207, 91 (1973).

67. R. A. Broglia, U. Gotz, M. Ichimura, T. Kammuri, and A. Winther, Phys. Letters 45B, 23 (1973).

68. A. Baltz and S. Kahana, Phys. Rev. Letters 29, 1267 (1942).

69. M. C. Lemaire, Physics Reports 7C, No. 6 (1973).

70. P. Bonche, Y. Cassagnou, H. Farragi, A. Jaffrin, R. Legrain, G. Morrison, and A. Papineau, Symposium on Heavy Ion Transfer Reactions (Argonne, 1973), p. 441.

71. A. Arima and V. Gillet, Ann. Phys. 66, 117 (1971), and references therein

72. A. Jaffrin, Nucl. Phys. A196, 577 (1972).

73. P. Bonche and B. Giraud, Phys. Rev. Letters 28, 1720 (1972); Nucl. Phys. A199, 160 (1973).

74. M. Ichimura, A. Arima, E. C. Halbert, and T. Teresawa, Nucl. Phys. A204, 225 (1973).

75. J. D. Garrett, Proceedings of the Symposium on Two Nucleon Transfer and Pairing Excitations (Argonne, 1972), p. 232.

76. A. Arima, R. A. Broglia, M. Ichimura, and K. Schafer, to be published.

77. G. J. Wozniak, H. L. Harney, K. H. Wilcox, and Joseph Cerny, Phys. Rev. Letters 28, 1278 (1972).

78. G. J. Wozniak, N. A. Jelley, and J. Cerny, Phys. Rev. Letters 31, 607 (1973).

79. D. Kurath, Phys. Rev. C7, 1390 (1973).

80. P. T. Debevec, H. J. Körner, and J. P. Schiffer, Phys. Rev. Letters 31, 171 (1973).

81. H. T. Fortune, Symposium on Heavy Ion Transfer Reactions (Argonne, 1973), p. 287.

82. R. Middleton, J. D. Garrett, and H. T. Fortune, Phys. Rev. Letters 27, 950 (1971).

83. N. Marquardt, W. von Oertzen, and R. L. Walter, Phys. Letters 35B, 37 (A71); K. Nagatani, M. J. Levine, T. A. Belote, and A. Arima, Phys. Rev. Letters 27, 1071 (1971).

84. T. A. Belote, N. Anyas-Weiss, J. A. Becker, J. C. Cornell, P. S. Fisher, P. N. Hudson, A. Menchaca-Rocha, A. D. Panagiotou, and D. K. Scott, Phys. Rev. Letters 30, 450 (1973).

85. D. Hanson, R. G. Stokstad, K. A. Erb, C. Olmer, and D. A. Bromley, to be published.

86. S. Cohen, F. Plasil, and W. J. Swiatecki, Lawrence Berkeley Laboratory Report LBL-1502, and references therein.

87. A. G. Artukh, G. F. Gridnev, V. I. Mikheev, V. V. Volkov, and J. Wilczynski, JINR Preprint E7-6970 and to be published.

88. J. Galin, D. Guerreau, M. Lefort, J. Peter, X. Tarrago, and R. Basile, Nucl. Phys. A159, 461 (1970).

89. P. J. Siemens, private communication.

90. H. Kamitsubo, M. Yoshie, I. Kohno, S. Nakajima, I. Yamane, and T. Mikumo, Symposium on Heavy Ion Transfer Reactions (Argonne, 1973), p. 549.

91. J. P. Bondorf and W. Norenberg, Phys. Letters 44B, 487 (1973).

92. C. Toepffer, Phys. Rev. Letters 27, 872 (1971).

93. J. P. Bondorf, F. Dickmann, D. H. E. Gross, and P. J. Siemens, J. de Physique C6, 145 (1971).

Table 1. Spectroscopic factors for the reaction $^{208}Pb(^{16}O,^{15}N)^{209}Bi$ at 104 MeV.

State / Method	$h_{9/2}$	$f^{*}_{7/2}$	$i_{13/2}$	$f_{5/2}$	$p_{3/2}$	$p_{1/2}$
No-Recoil (Ref. 30)	4.80	1.00	0.83	4.00	1.15	3.50
Nagarajan (Ref. 30)	1.32	1.00	0.80	1.12	1.28	0.82
Tamura (Ref. 27)	1.29	1.00	--	0.92	0.79	0.61
Semi-Classical (Ref. 28)	0.71	1.00	1.12	1.10	1.26	0.78

*Spectroscopic factors are normalized to unity for $f_{7/2}$ state.

Table 2. Characteristic parameters in heavy ion reactions.

Reaction	E	η	kR	θ_C^*	$\delta\theta_C^{**}$	$\delta\theta_D^{***}$
$^{12}C + ^{208}Pb$	114	25	100	29°	10°	1.8°
$^{14}N + ^{48}Ca$	50	16	43	43°	10°	4.5°
$^{12}C + ^{12}C$	114	1.8	30	7°	9°	6°

*Evaluated from Eq. (1).

**Evaluated from Eq. (3).

***Spacing of diffraction oscillations (π/kR).

Table 3. Comparison of experimental cross sections for the $^{12}C(^{12}C,^{9}Be)^{15}O$ reaction at 114 MeV with theoretical cross sections evaluated using a semi-classical theory for the reaction mechanism and three nucleon cluster spectroscopic amplitudes.

State in ^{15}O	σ_{Theory}	$\sigma_{Expt.}$
g.s. $1/2^-$	0.01	≈ 0
5.24, $5/2^+$	0.10	0.12
6.79, $3/2^+$	0.003	≈ 0
7.28, $7/2^+$	0.33	0.28
(9.08)[a], $9/2^+$	0.76	?
(10.8)[a], $7/2^+$	0.29	?
12.89[c], $11/2^-$	1.00[b]	1.00
15.36[c], $13/2^+$	2.16	1.16

[a] Theoretical excitation energy.

[b] Data normalized to unity for 12.89 state.

[c] Excitation energy taken from Fig. 8; these states were identified with $11/2^-$ and $13/2^+$ from their strong excitation.

FIGURE CAPTIONS

Fig. 1. (a) Energy spectrum for the $^{208}Pb(^{12}C,^{11}B)^{209}Bi$ reaction at 78 MeV, showing the selective excitation of single particle states. (b) The ratio of cross sections for $j = \ell + 1/2$ and $j = \ell - 1/2$ states in several nuclei, excited by the $(^{16}O,^{15}N)$ and $(^{12}C,^{11}B)$ reactions.

Fig. 2. (a) differential cross sections for the $^{208}Pb(^{12}C,^{13}C)^{207}Pb$ reaction leading to single-hole states at incident energies of 77, 98 and 116 MeV. The bold arrows denote the grazing angle predicted by Eq. (1). The locus of this angle as a function of excitation energy is also indicated. The bold horizontal lines are the minimum FWHM of the distributions predicted from Eq. (3).

(b) differential cross sections for the $^{208}Pb(^{12}C,^{11}B)^{209}Bi$ reaction at 78 MeV. The dotted lines are drawn through the data points, and the solid curves are DWBA theory predictions.

Fig. 3. Vector diagram for the reaction A(a,b)B with a = b + x and B = A + x. The relative coordinates of the colliding nuclei in the initial and final channels are $\underline{r}_i$, $\underline{r}_f$, and $\underline{r}$ is relative coordinate of the cores. The coordinate of the transferred particle x in the incident and residual nuclei is represented by $\underline{r}_1$, $\underline{r}_2$.

Fig. 4. Theoretical calculation of the Q-dependence for the $^{208}Pb(^{16}O,^{15}N)^{209}Bi$ reaction using (a) DWBA theory and (b) semiclassical theory. In (a) the form factor ($F(\underline{r})$ in Eq. (7)) was calculated with the binding energy of the state fixed at the value for the actual single particle level, whereas in (b) the binding energy was allowed to change with Q-value.

Fig. 5. (a) Mass spectrum obtained from "time-of-flight" in reactions with $^{28}Si + ^{28}Si$. (b) Differential cross sections for the $^{29}Si(^{28}Si,^{28}Si)^{29}Si$ reaction. The solid curve is the optical model prediction including the contribution from "elastic transfer".

Fig. 6. Differential cross sections for the reaction $^{48}Ca(^{14}N,^{13}C)^{49}Sc$. The solid curves are DWBA predictions including recoil effects.

Fig. 7. Differential cross section for the $^{13}C(^{12}C,^{13}C)^{12}C$ reaction at 87 MeV. The dashed curve is the DWBA prediction excluding recoil effects ($\ell = 0$ transfer only). The solid line shows the effect of including recoil which damps the oscillations by allowing $\ell = 1$ in addition to $\ell = 0$ transfer.

Fig. 8. Energy spectra for the $^{12}C(^{10}B,^{7}Li)^{15}O$ and $^{12}C(^{10}B,^{7}Be)^{15}N$ reactions at 100 MeV, indicating the marked selectivity of heavy-ion transfer reactions on light nuclei.

Fig. 9. Energy variation of the transition probability to different final states in the reaction $^{12}C(^{12}C,^{9}Be)^{15}O$, predicted by semiclassical theory. High-spin states are enhanced at high energy, due to the increasing effects of recoil.

Fig. 10. Energy spectra for the $^{12}C(^{12}C,^{9}Be)^{15}O$ reaction at 72, 114 and 174 MeV.

Fig. 11. Illustration of direct and indirect routes in transfer reactions.

Fig. 12. Differential cross sections for the $^{40}Ca(^{18}O,^{20}Ne)^{38}Ar$ reaction (the J^{π} values in brackets refer to ^{20}Ne, ^{38}Ar states). In (a) the data are compared with DWBA predictions (solid lines). (b) illustrates the CCBA predictions which partly reproduce the forward rise of the differential cross section for the $(2^+,0^+)$ channel. The bottom figure is a pictorial representation as discussed in the text.

Fig. 13. Comparison of data for the reaction $^{120}Sn(^{18}O,^{16}O)^{122}Sn$ at 100 MeV with DWBA and CCBA calculations (the two theories give almost identical results for the ground state (0^+) excitation). The data illustrate the strong enhancement in the excitation of the (0^+) pairing vibration over the (2^+) collective vibration.

Fig. 14. Transfer probabilities $P_{tr}(d_o)$ for $(^{16}O,^{14}C)$ reactions or various target nuclei, deduced using semiclassical models. The reactions on Ce, Nd and Sm are enhanced by a factor of order 20-30.

Fig. 15. (a) Theoretical spectrum calculated using the aligned scheme for the four-nucleon configurations, and the generator-coordinate DWBA formalism.

(b) Energy spectrum for the $^{90}Zr(^{16}O,^{12}C)^{94}Mo$ reaction.

Fig. 16. Energy spectra for the reactions $^{11}B(\alpha,^{7}Li)^{8}Be$ and $^{11}B(\alpha,^{8}Be)^{7}Li$ ((a) and (b)) showing the complete separation of ^{8}Be and ^{7}Li. (c) Spectrum for $^{16}O(\alpha,^{8}Be)^{12}C$; the ^{8}Be line in the spectrum comes from the reaction on a ^{12}C contaminant.

Fig. 17. (a) Experimental arrangement for detecting ^{8}Be by means of the position signal produced in the central region of the position sensitive detector by the decay α-particles. Particle stable nuclei are eliminated by the central post of the divided collimator.

(b) Particle identifier spectrum gated by position signals from region x_2 (particle stable nuclei) and x (α's from ^{8}Be decay).

Fig. 18. (a) Energy spectrum for the $^{12}C(^{12}C,\alpha)^{20}Ne$ reaction, showing the selective excitation of the 7.833 MeV (2^+) state relative to the 7.421 MeV state. Similar selectivity is observed in the (0^+) states at 7.195 and 6.722 MeV. (b) Excitation functions for several states; the fluctuations in the 7.83 MeV state are superimposed on a direct background.

Fig. 19. Angular distributions for the $^{14}N + ^{12}C \rightarrow ^{6}Li + ^{20}Ne$ reaction. The forward angles were measured using the $^{12}C(^{14}N, ^{6}Li)^{20}Ne$ reaction and the backward angles using the $^{14}N(^{12}C, ^{6}Li)^{20}Ne$ reaction at the same centre of mass energy. The solid lines are theoretical predictions using Hauser-Feshbach theory.

Fig. 20. Contours of equal $d^2\sigma/d\Omega dQ$ for the $^{232}Th(^{40}Ar, ^{39}K)$ reaction at 380 MeV.

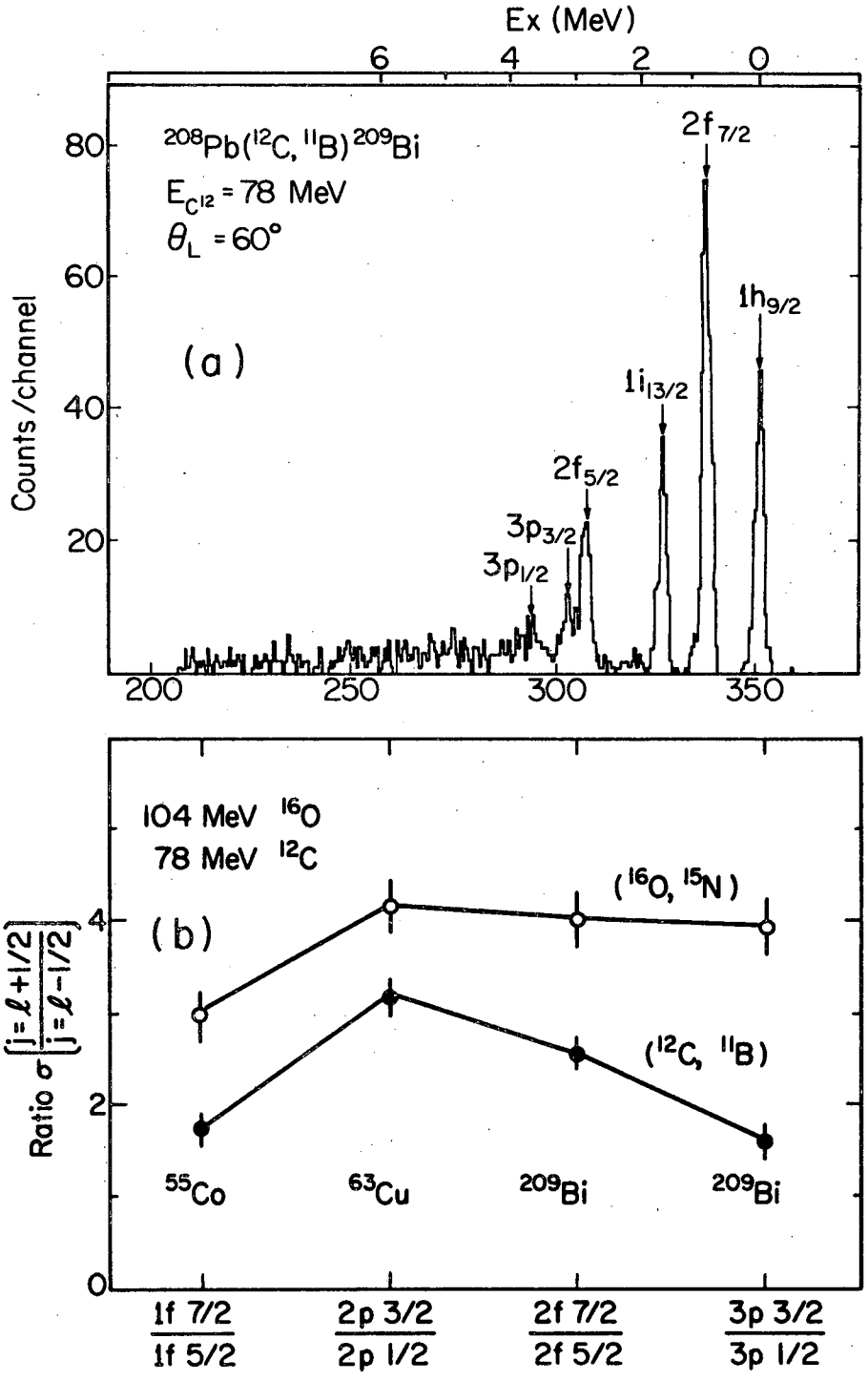

XBL738-3777

Fig. 1

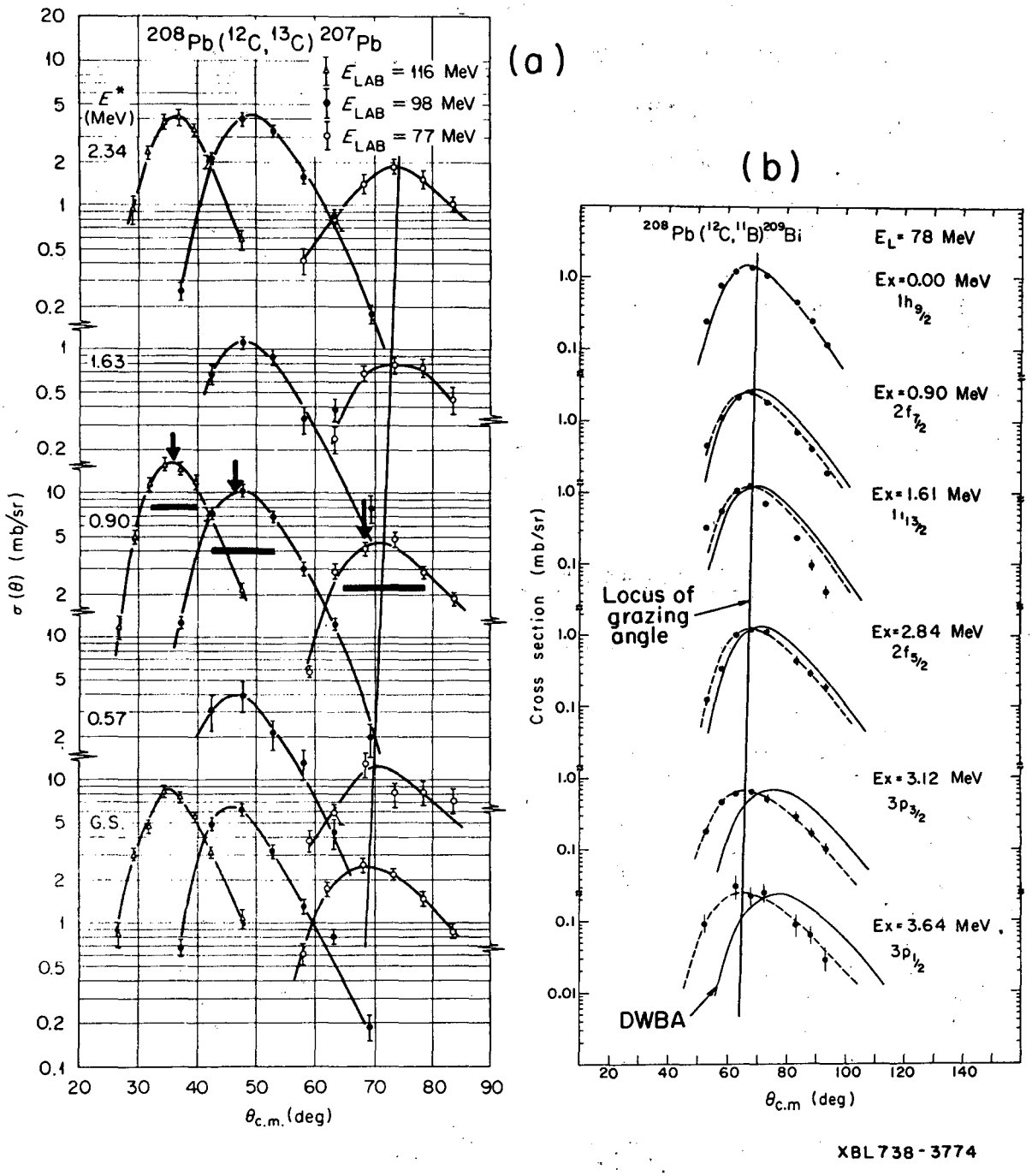
(a)
$^{208}Pb(^{12}C,^{13}C)^{207}Pb$
E_{LAB} = 116 MeV
E_{LAB} = 98 MeV
E_{LAB} = 77 MeV
E^* (MeV)
2.34
1.63
0.90
0.57
G.S.
$\sigma(\theta)$ (mb/sr)
$\theta_{c.m.}$ (deg)
(b)
$^{208}Pb(^{12}C,^{11}B)^{209}Bi$
E_L = 78 MeV
Ex=0.00 MeV
$1h_{9/2}$
Ex=0.90 MeV
$2f_{7/2}$
Ex=1.61 MeV
$1i_{13/2}$
Locus of grazing angle
Ex=2.84 MeV
$2f_{5/2}$
Ex=3.12 MeV
$3p_{3/2}$
Ex=3.64 MeV
$3p_{1/2}$
DWBA
Cross section (mb/sr)
$\theta_{c.m}$ (deg)
XBL738-3774

Fig. 2

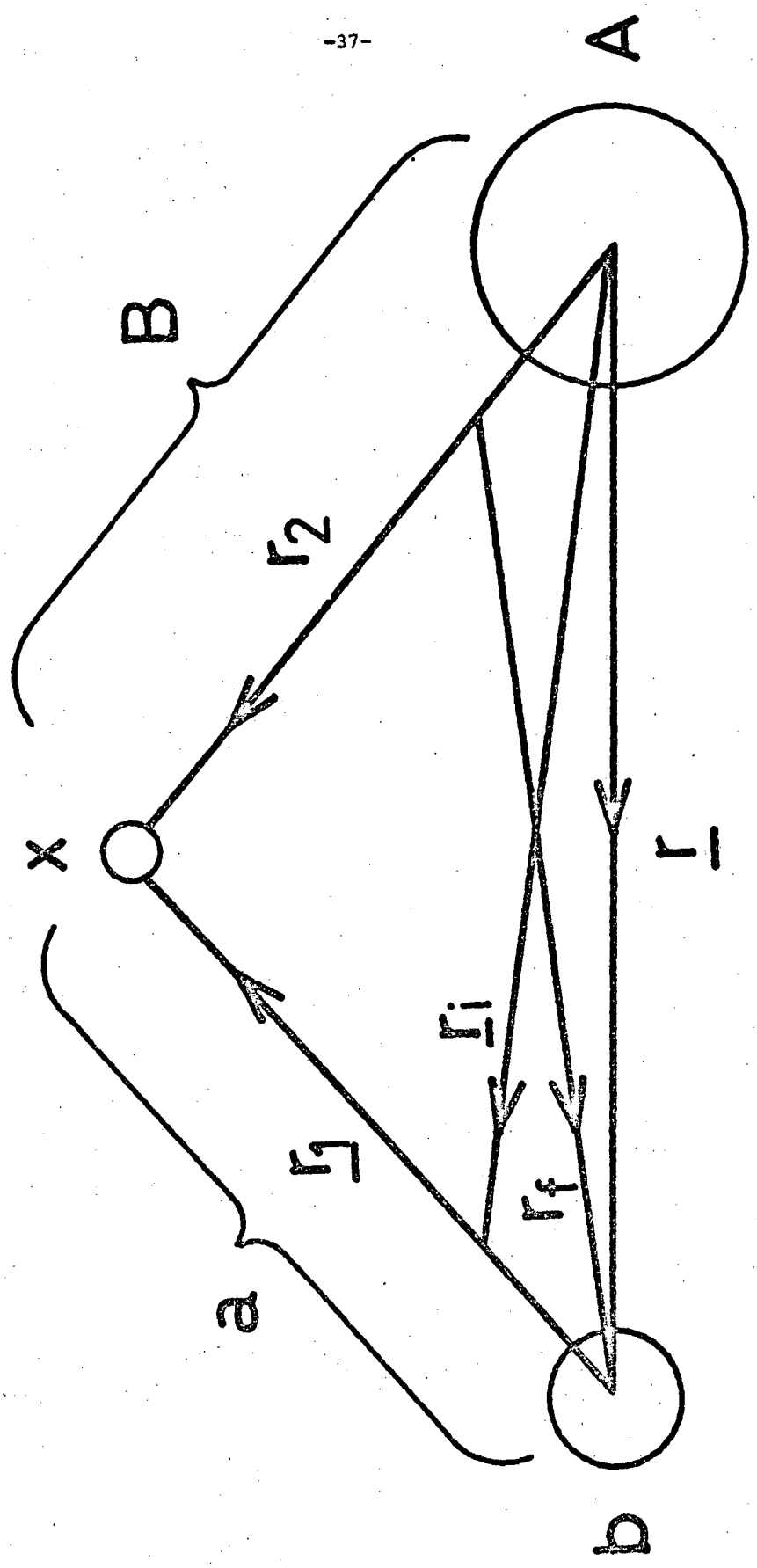

Fig. 3

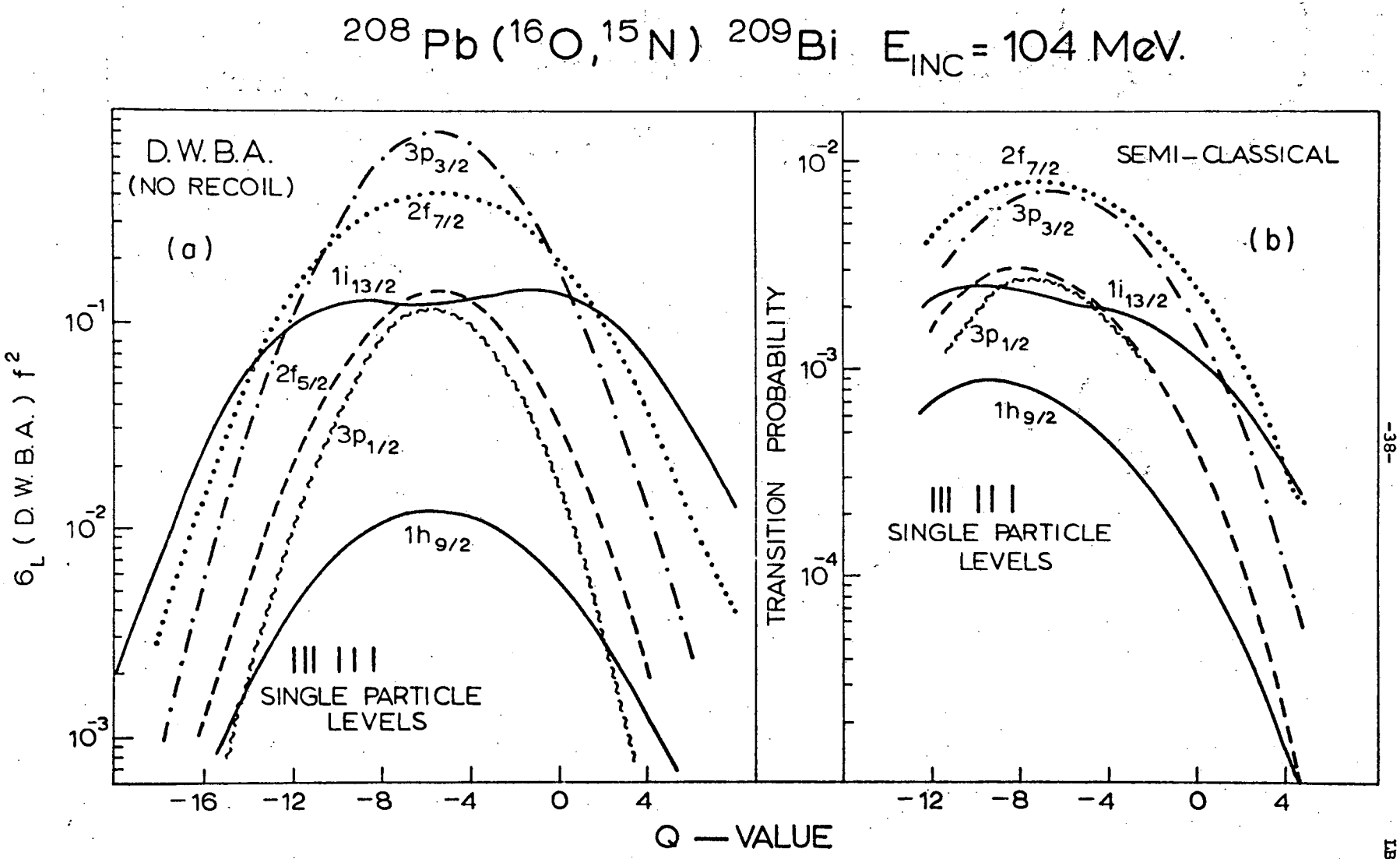

Fig. 4

LBL-1691

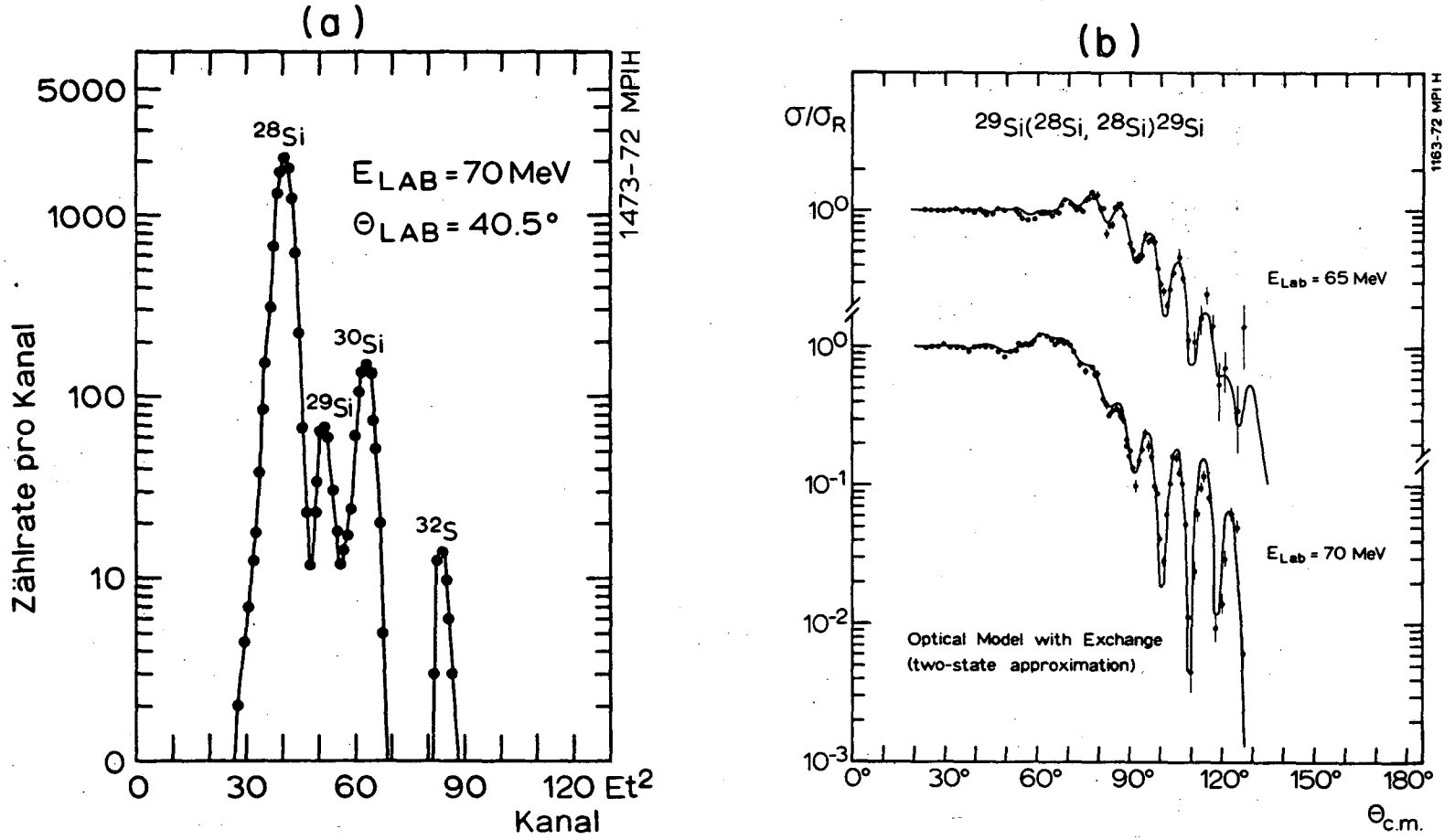

XBL738-3770

Fig. 5

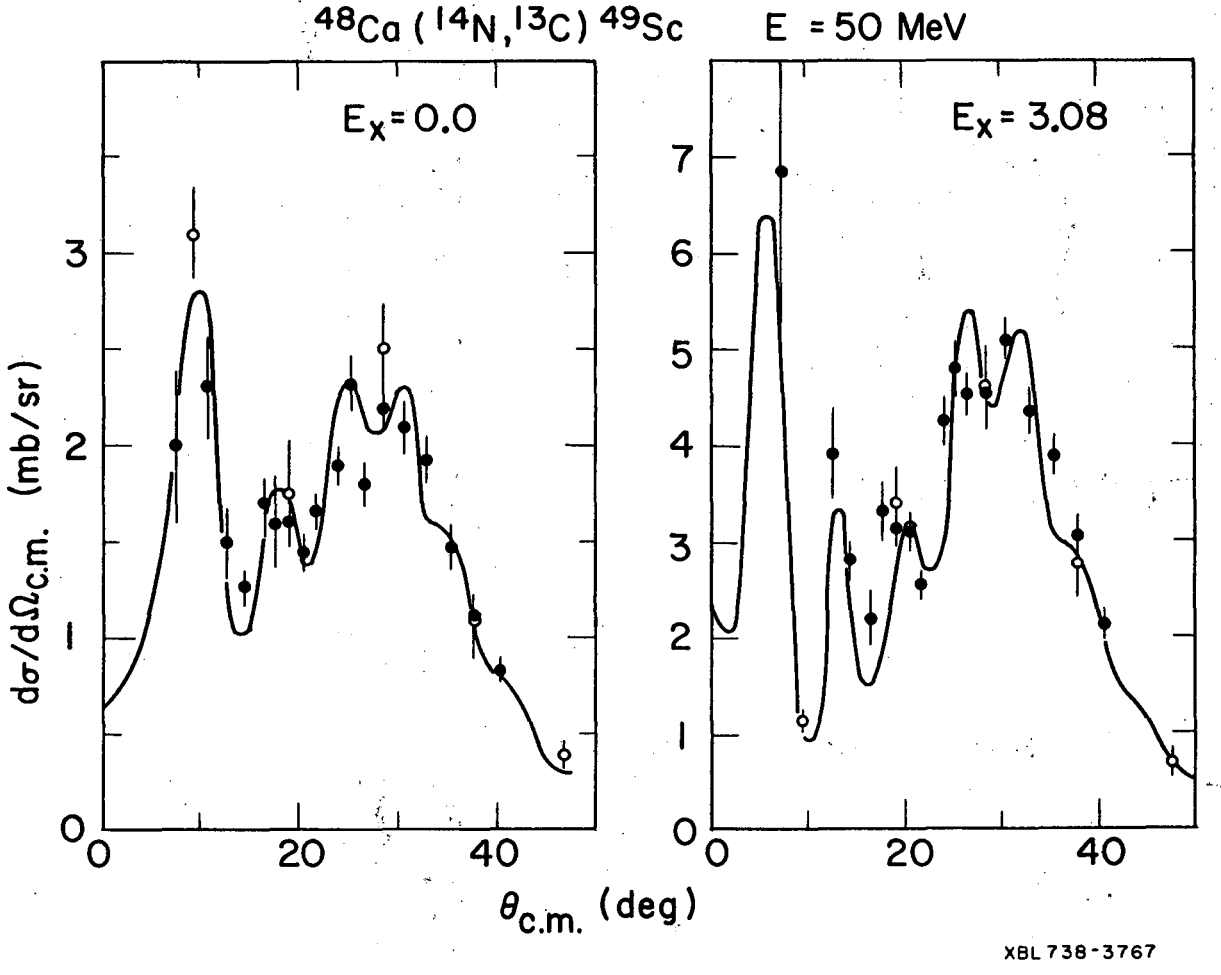
$^{48}Ca\,(^{14}N,^{13}C)\,^{49}Sc$ E = 50 MeV
E_x = 0.0
E_x = 3.08
$d\sigma/d\Omega_{c.m.}$ (mb/sr)
$\theta_{c.m.}$ (deg)
0
20
40
1
2
3
4
5
6
7
XBL 738-3767

Fig. 6

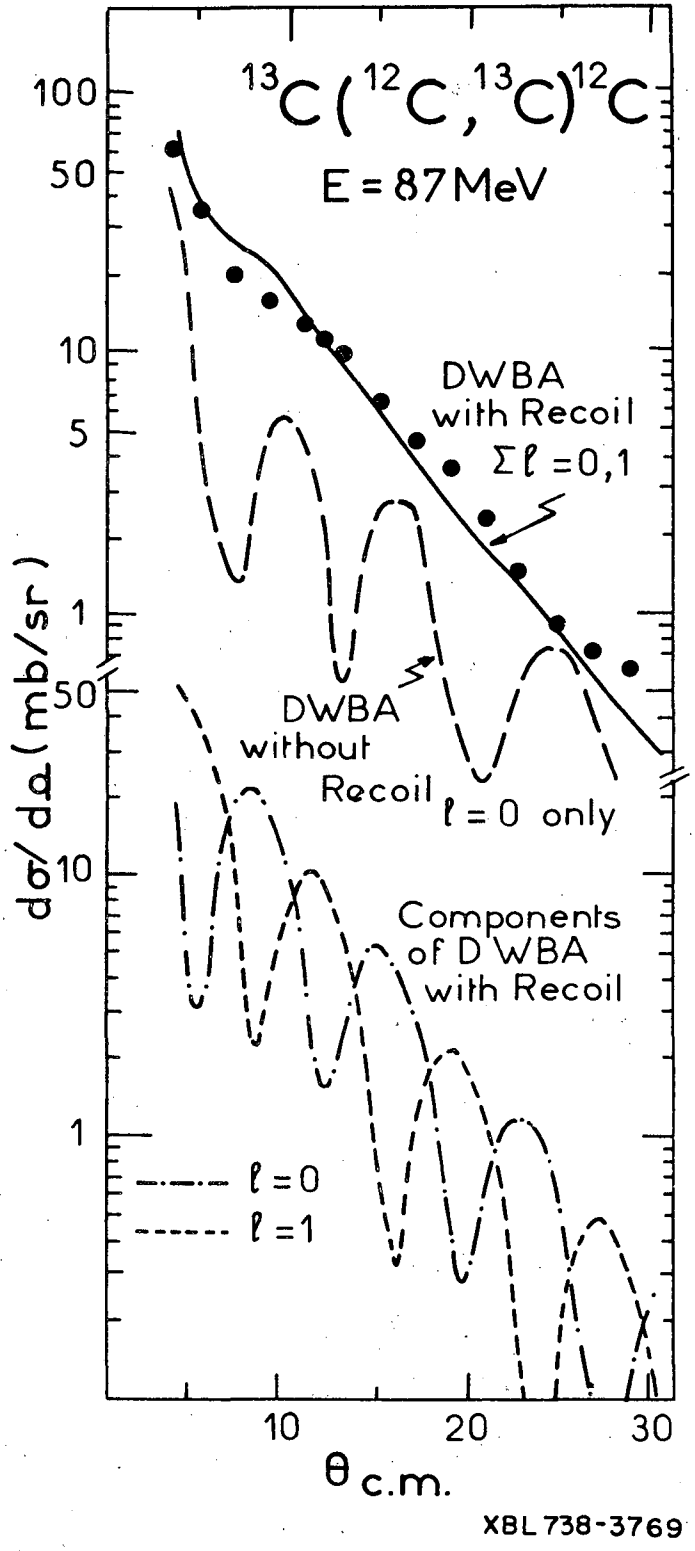
$^{13}C(^{12}C,^{13}C)^{12}C$
E = 87 MeV
DWBA
with Recoil
Σℓ =0,1
DWBA
without
Recoil
ℓ = 0 only
Components
of DWBA
with Recoil
ℓ =0
ℓ =1
dσ/dΩ (mb/sr)
θ c.m.
100
50
10
5
1
50
10
1
10
20
30
XBL 738-3769

Fig. 7

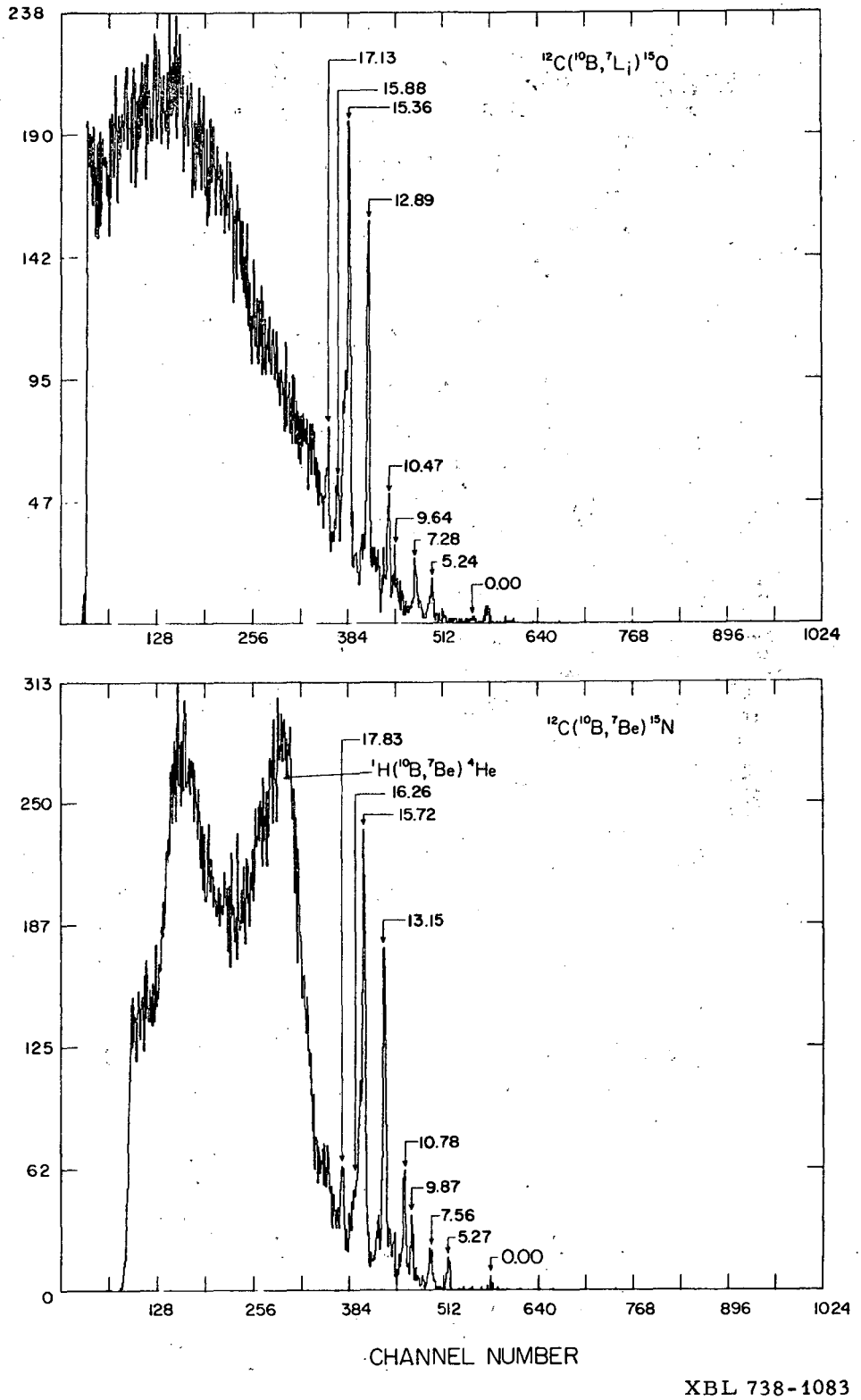

XBL 738-1083

Fig. 8

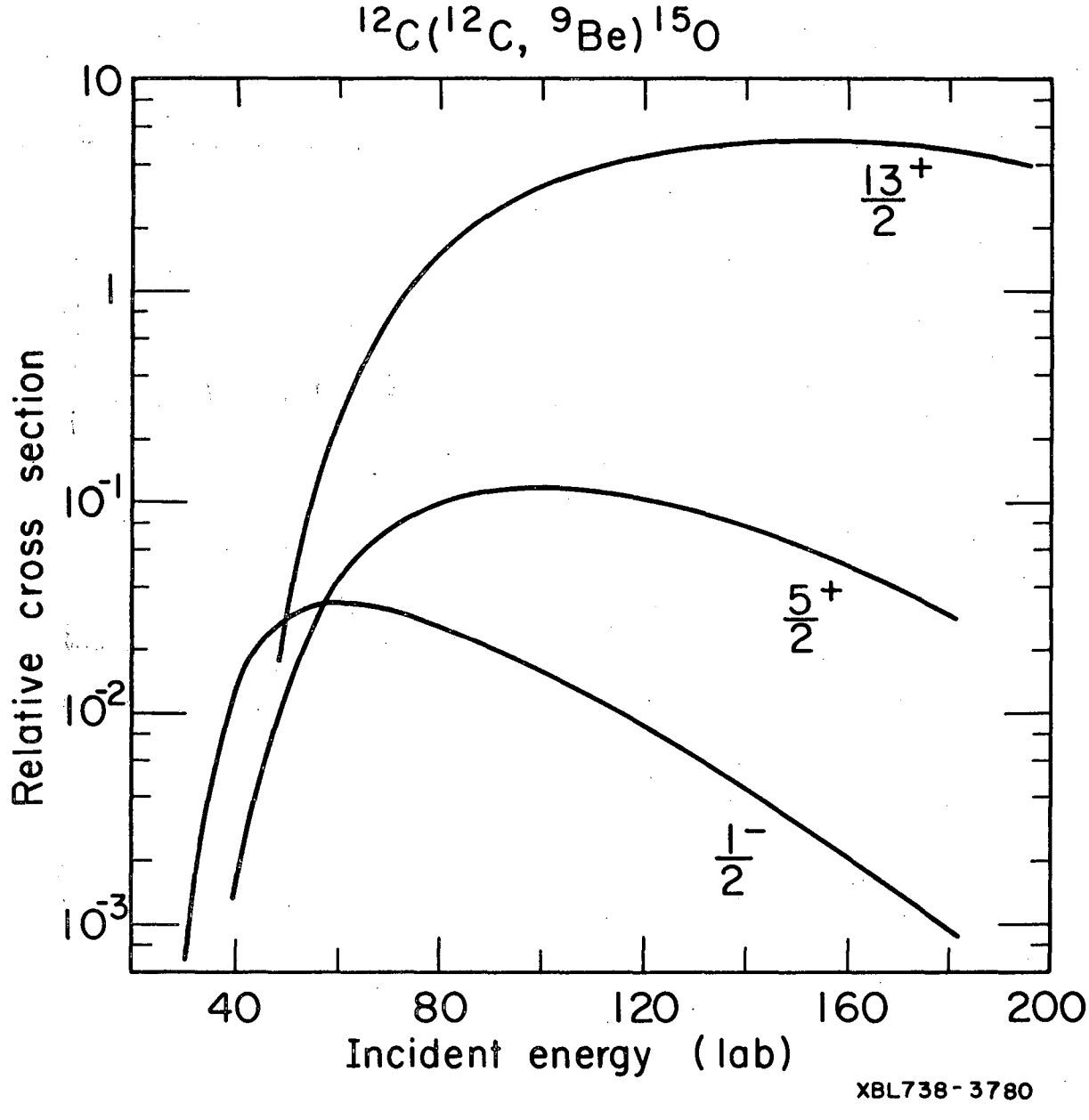
$^{12}C(^{12}C, ^{9}Be)^{15}O$
Relative cross section
10
1
10^{-1}
10^{-2}
10^{-3}
$\frac{13^+}{2}$
$\frac{5^+}{2}$
$\frac{1^-}{2}$
40
80
120
160
200
Incident energy (lab)
XBL738-3780

Fig. 9

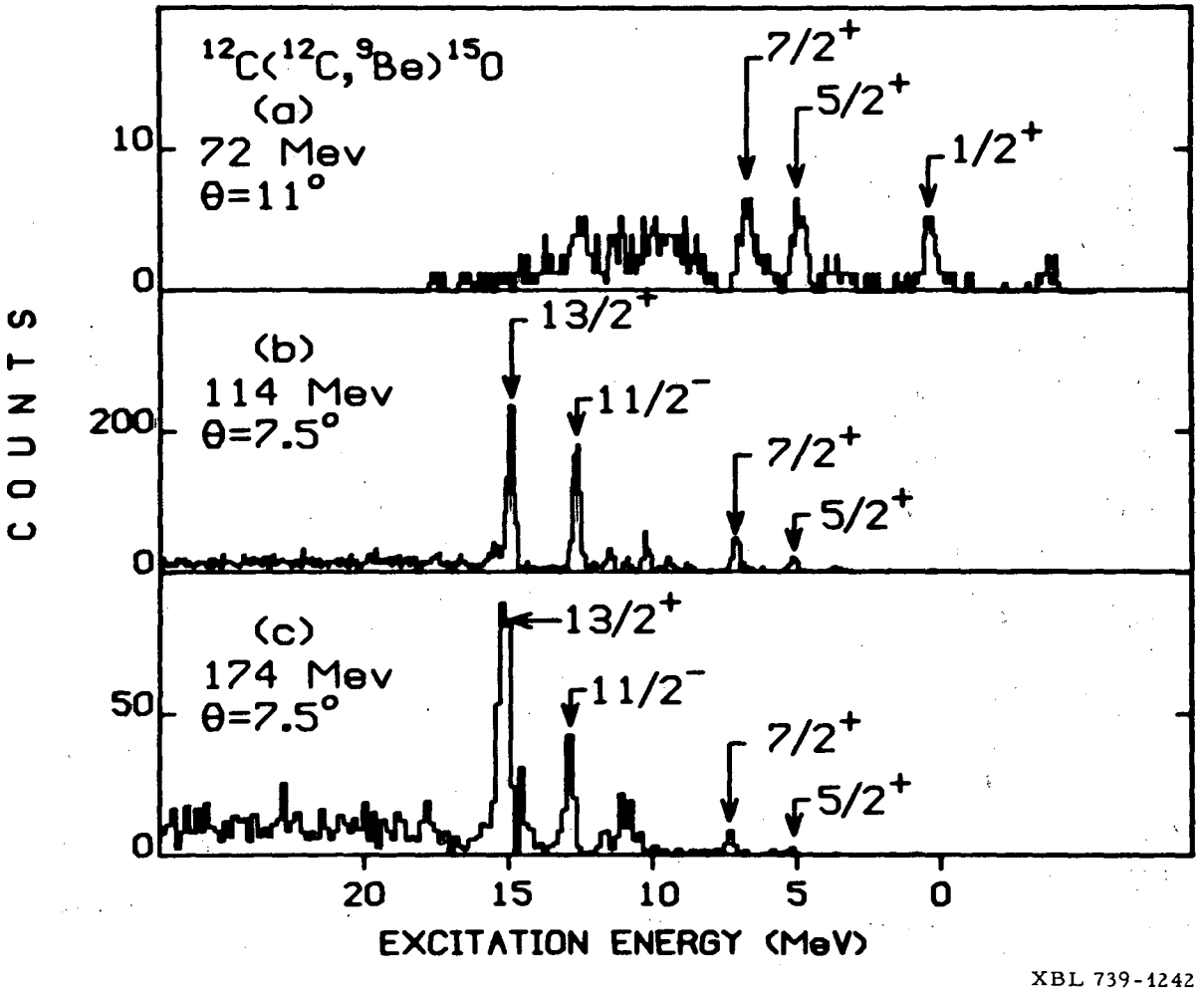

XBL 739-1242

Fig. 10

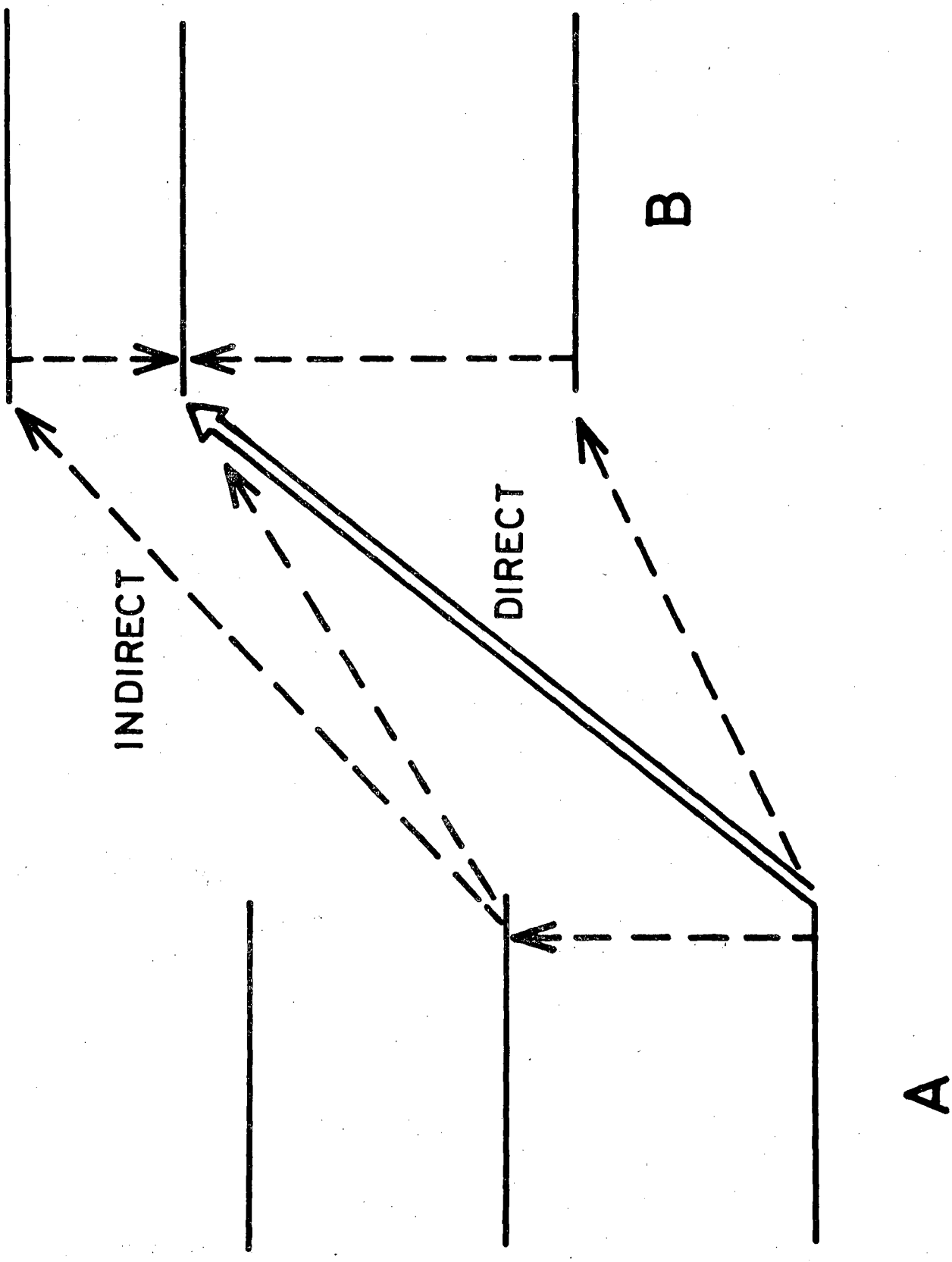

Fig. 11

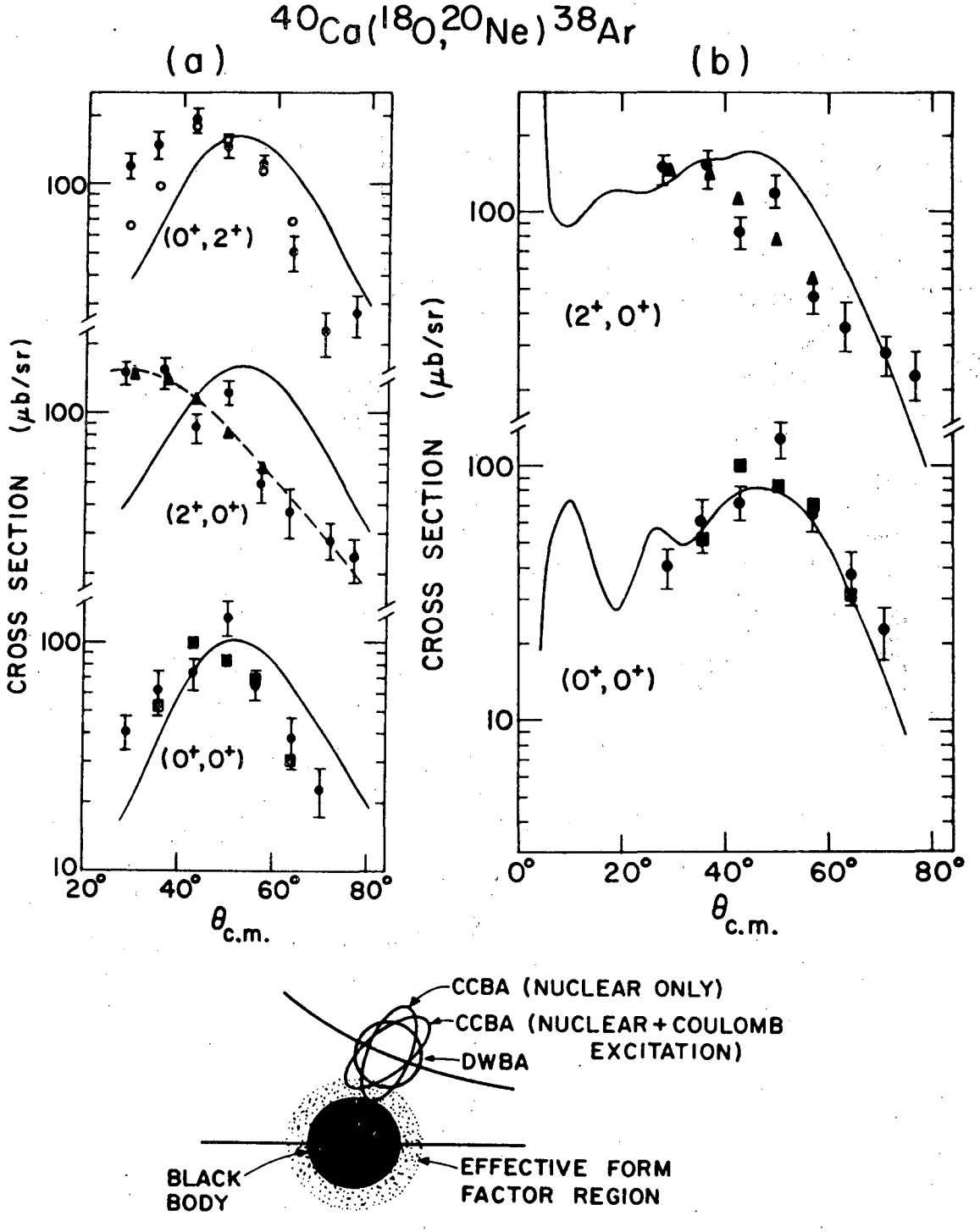
$^{40}Ca(^{18}O,^{20}Ne)^{38}Ar$
(a)
(b)
CROSS SECTION (μb/sr)
100
10
(0⁺,2⁺)
(2⁺,0⁺)
(0⁺,0⁺)
20°
40°
60°
80°
0°
θc.m.
CCBA (NUCLEAR ONLY)
CCBA (NUCLEAR + COULOMB EXCITATION)
DWBA
BLACK BODY
EFFECTIVE FORM FACTOR REGION
XBL738-3776

Fig. 12

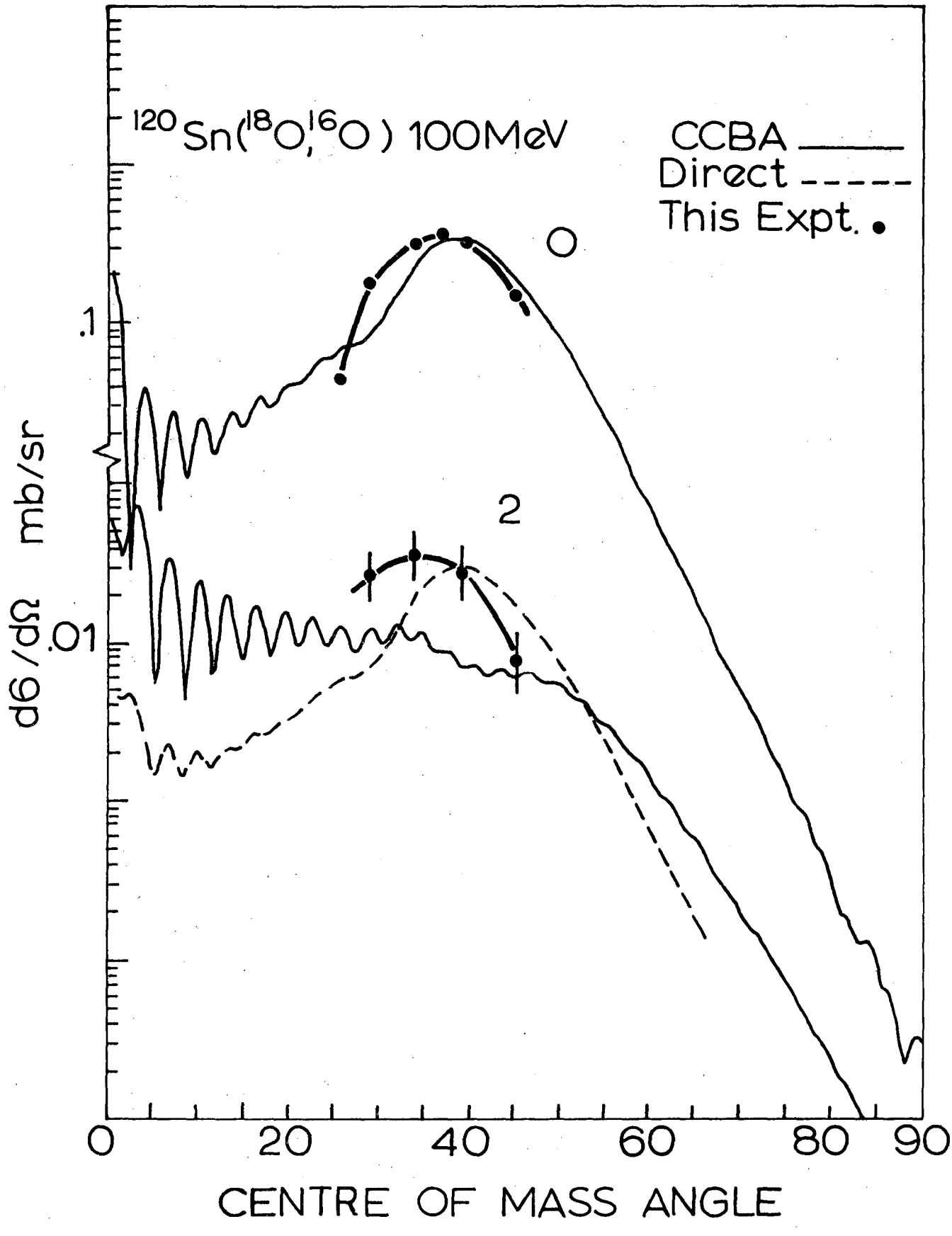
$^{120}Sn(^{18}O,^{16}O)$ 100MeV
CCBA
Direct
This Expt.
0
2
.1
.01
dσ/dΩ mb/sr
0
20
40
60
80
90
CENTRE OF MASS ANGLE

Fig. 13

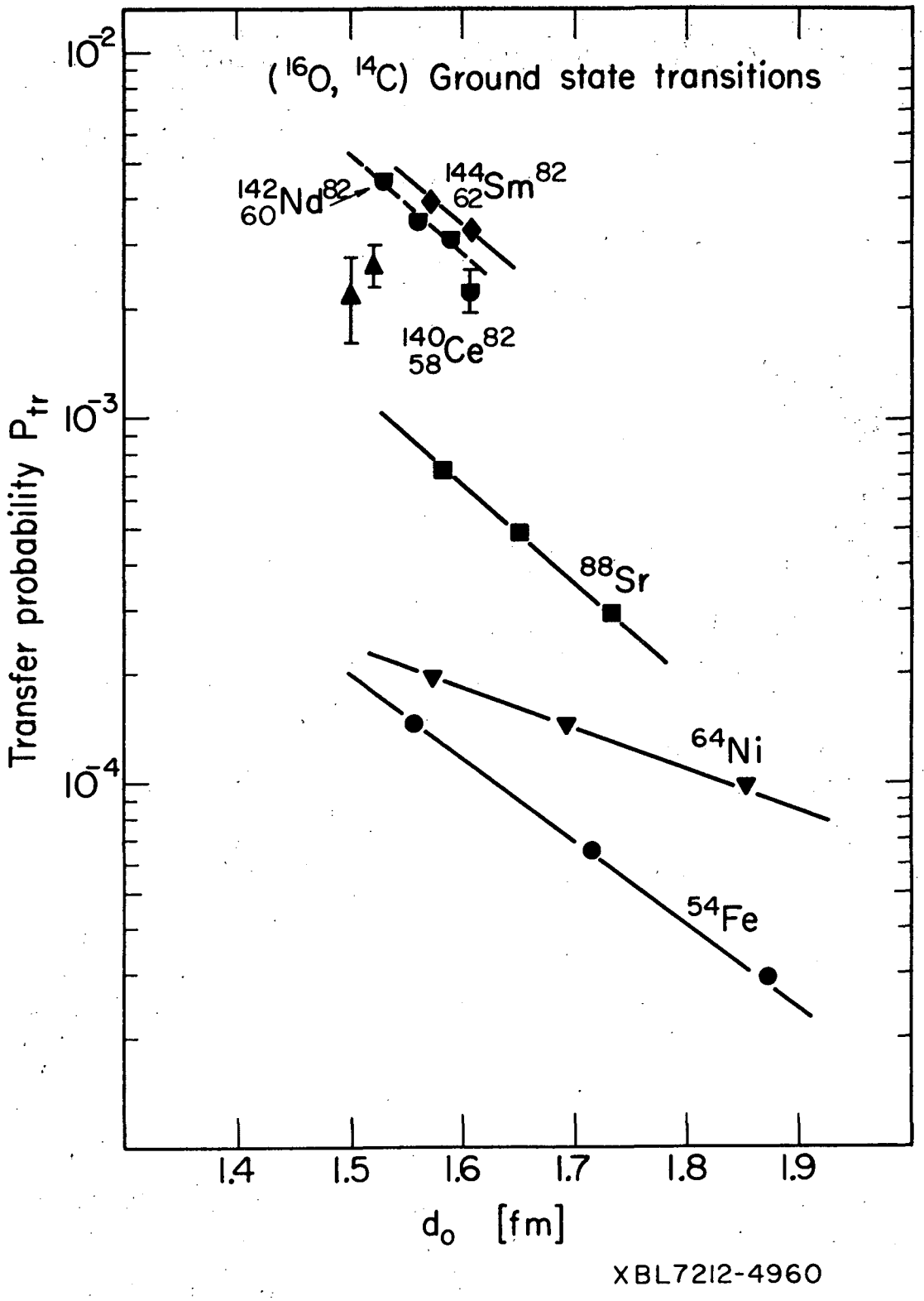
(^{16}O, ^{14}C) Ground state transitions
$^{142}_{60}$Nd^{82}
$^{144}_{62}$Sm^{82}
$^{140}_{58}$Ce^{82}
^{88}Sr
^{64}Ni
^{54}Fe
Transfer probability P_{tr}
10^{-2}
10^{-3}
10^{-4}
1.4
1.5
1.6
1.7
1.8
1.9
d_o [fm]
XBL7212-4960

Fig. 14

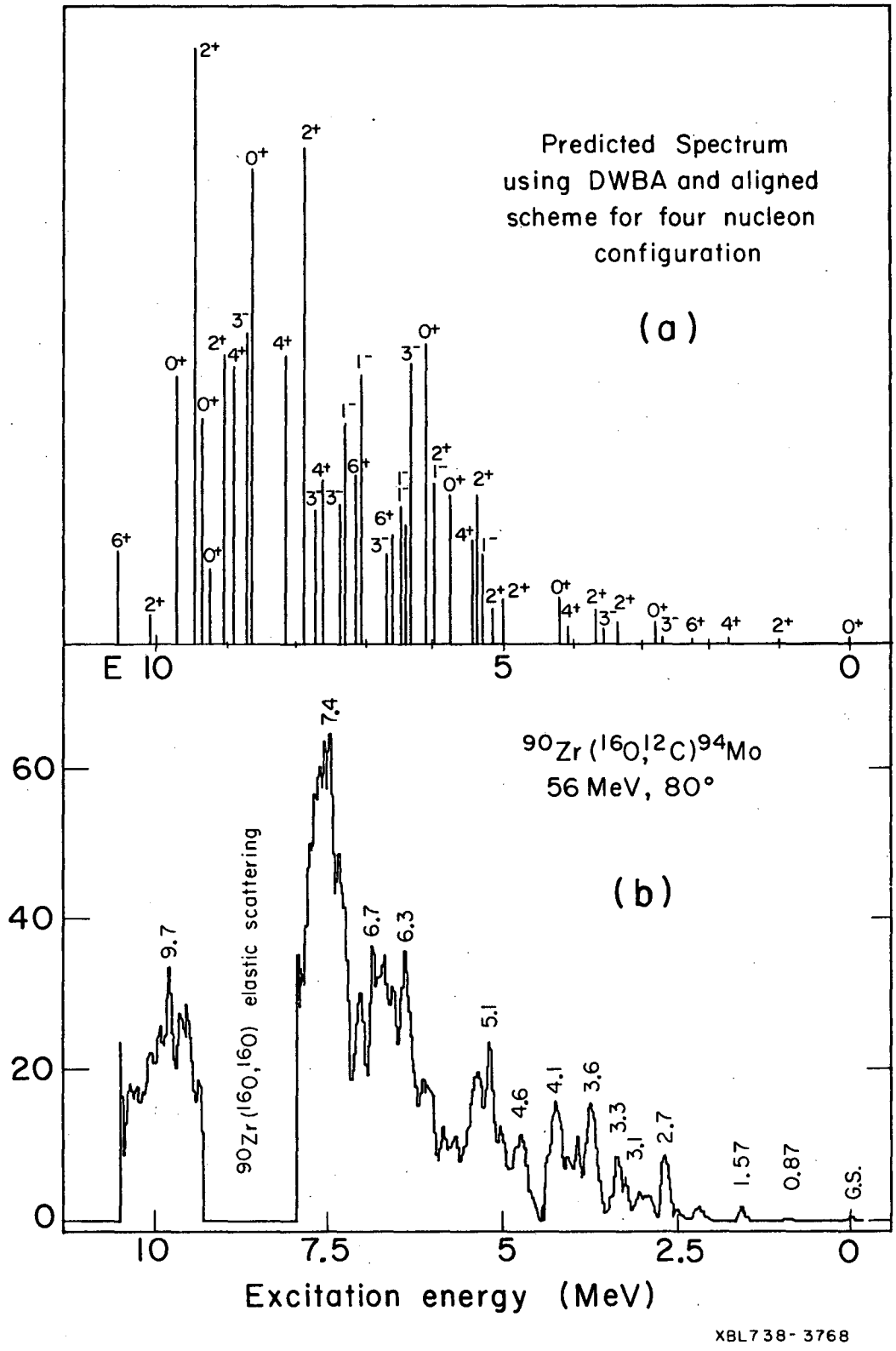
Predicted Spectrum
using DWBA and aligned
scheme for four nucleon
configuration
(a)
E 10
5
0
$^{90}Zr(^{16}O,^{12}C)^{94}Mo$
56 MeV, 80°
(b)
$^{90}Zr(^{16}O,^{16}O)$ elastic scattering
9.7
7.4
6.7
6.3
5.1
4.6
4.1
3.6
3.3
3.1
2.7
1.57
0.87
G.S.
60
40
20
0
10
7.5
5
2.5
0
Excitation energy (MeV)
XBL738-3768

Fig. 15

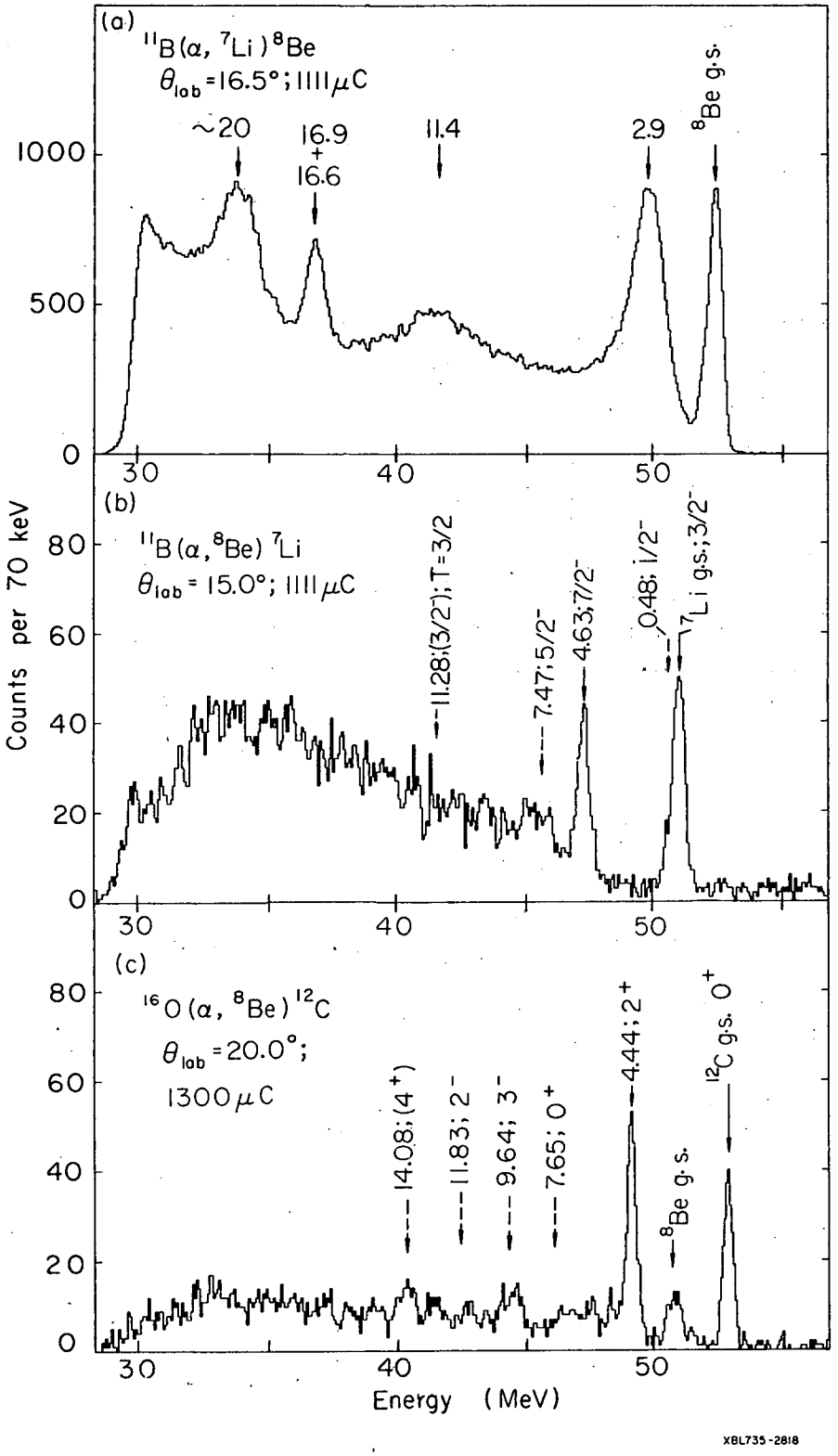
(a)
$^{11}B(\alpha, ^{7}Li)^{8}Be$
θ_{lab}=16.5°; 1111μC
~20
16.9
+
16.6
11.4
2.9
^{8}Be g.s.
1000
500
0
30
40
50
(b)
$^{11}B(\alpha, ^{8}Be)^{7}Li$
θ_{lab} = 15.0°; 1111μC
11.28;(3/2); T=3/2
7.47;5/2⁻
4.63;7/2⁻
0.48; 1/2⁻
^{7}Li g.s.;3/2⁻
Counts per 70 keV
80
60
40
20
0
30
40
50
(c)
$^{16}O(\alpha, ^{8}Be)^{12}C$
θ_{lab} = 20.0°;
1300μC
14.08;(4⁺)
11.83; 2⁻
9.64; 3⁻
7.65; 0⁺
4.44; 2⁺
^{8}Be g.s.
^{12}C g.s. 0⁺
80
60
40
20
0
30
40
50
Energy (MeV)
XBL735-2818

Fig. 16

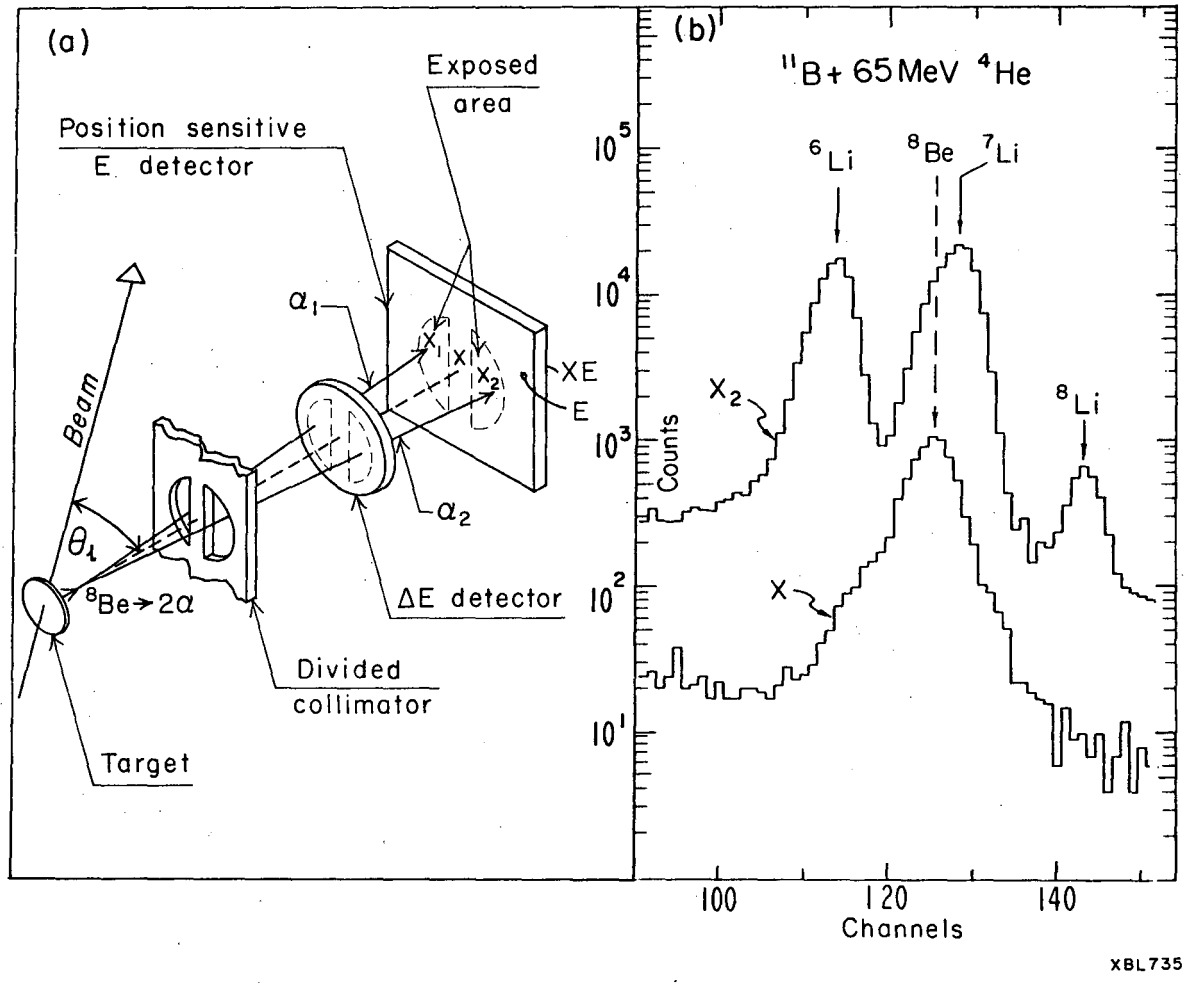
(a)
Exposed
area
Position sensitive
E detector
Beam
α_1
θ_1
$^8Be \rightarrow 2\alpha$
α_2
XE
E
ΔE detector
Divided
collimator
Target
(b)
$^{11}B + 65MeV\ ^4He$
^6Li
^8Be
^7Li
^8Li
X_2
X
Counts
10^5
10^4
10^3
10^2
10^1
100
120
140
Channels
XBL735-2817

Fig. 17

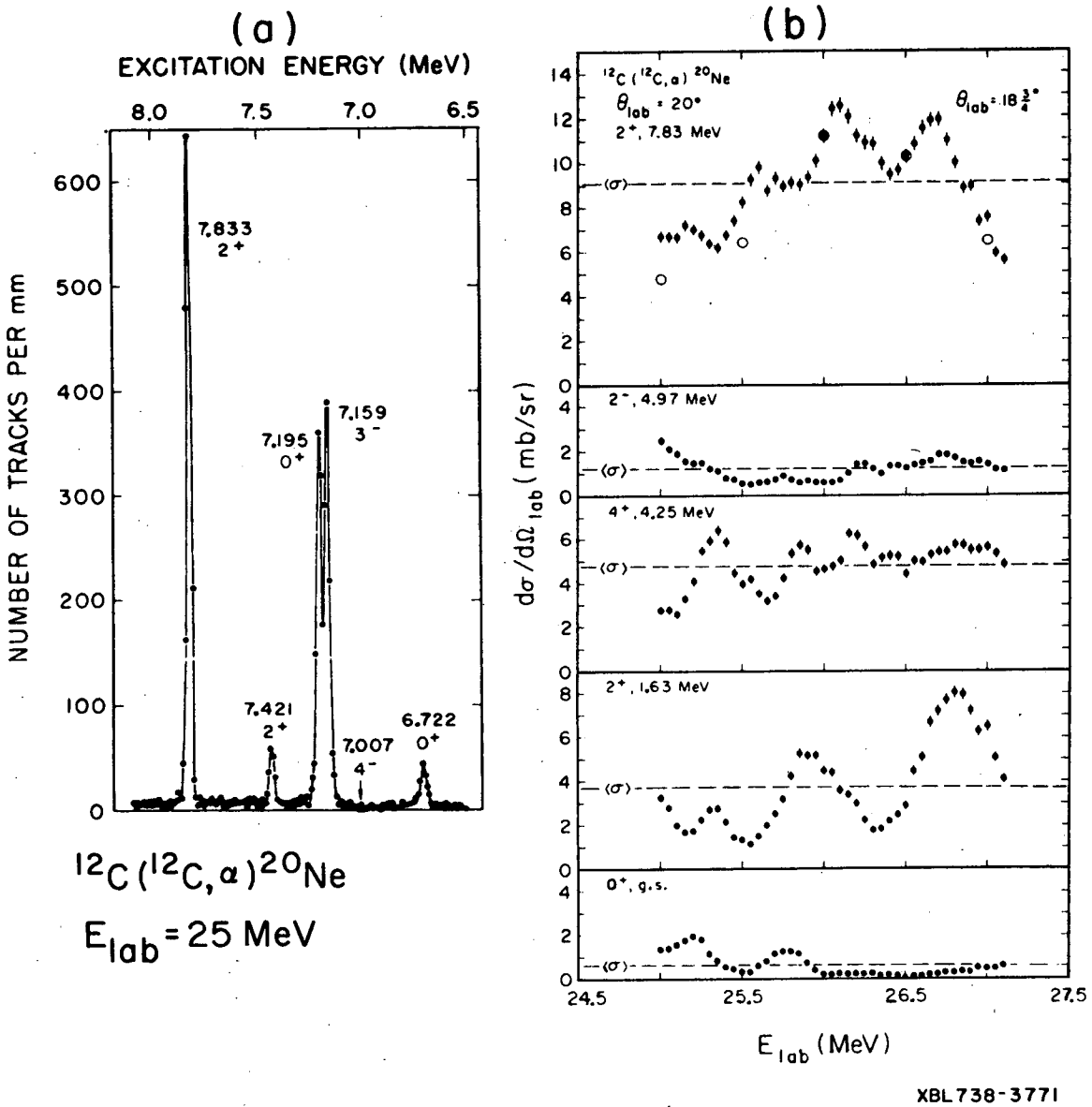
(a)
EXCITATION ENERGY (MeV)
8.0
7.5
7.0
6.5
NUMBER OF TRACKS PER mm
600
500
400
300
200
100
0
7.833
2+
7.195
0+
7.159
3-
7.421
2+
7.007
4-
6.722
0+
12C(12C,α)20Ne
Elab = 25 MeV
(b)
12C(12C,α)20Ne
θlab = 20°
2+, 7.83 MeV
θlab = 18 3/4°
(σ)
2-, 4.97 MeV
4+, 4.25 MeV
2+, 1.63 MeV
0+, g.s.
dσ/dΩlab (mb/sr)
24.5
25.5
26.5
27.5
Elab (MeV)
XBL738-3771

Fig. 18

The Reactions $^{12}C(^{14}N,^{6}Li)^{20}Ne$ and $^{14}N(^{12}C,^{6}Li)^{20}Ne$ at $E_{c.m.} = 36$ MeV

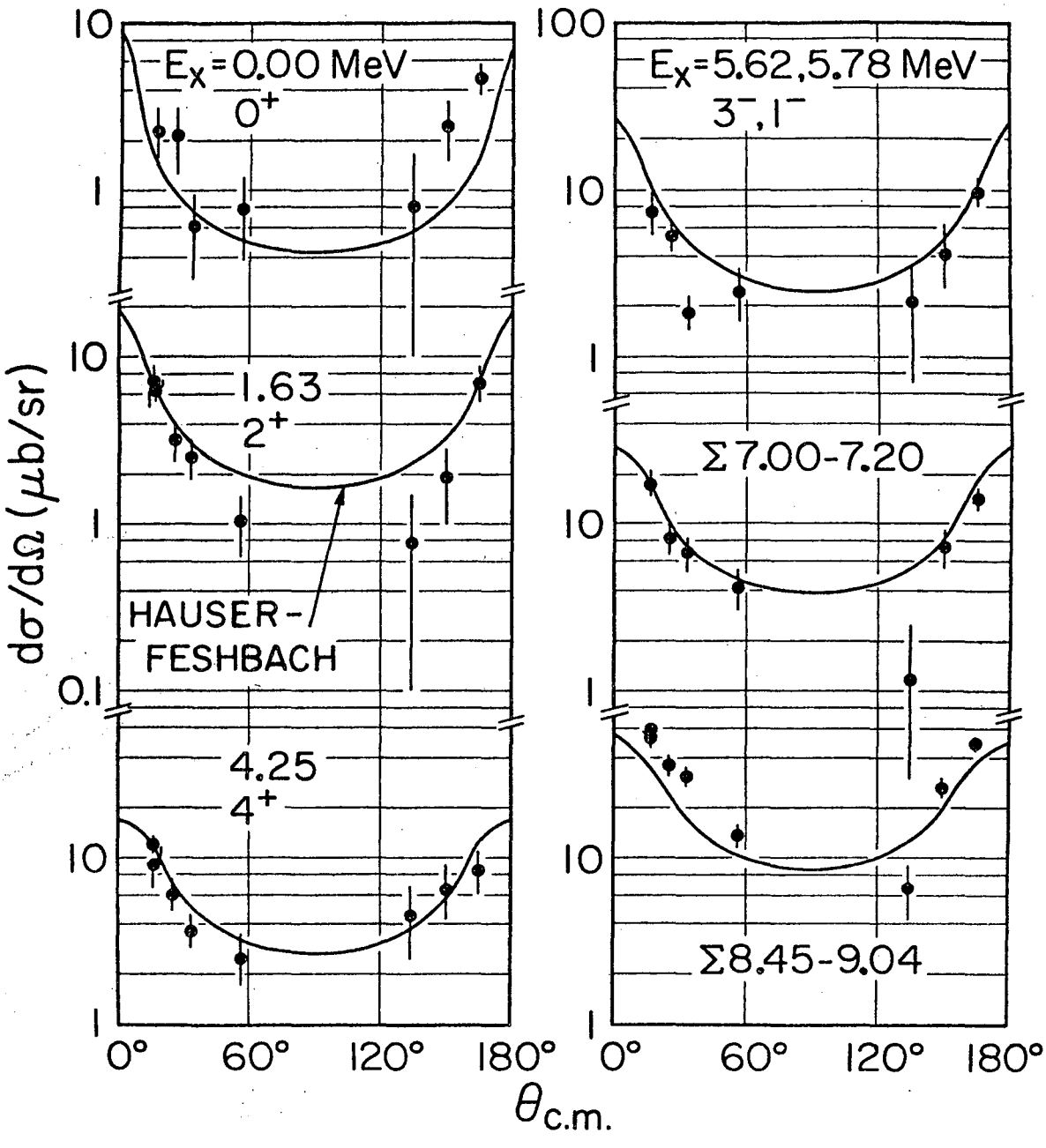

XBL738-3772

Fig. 19

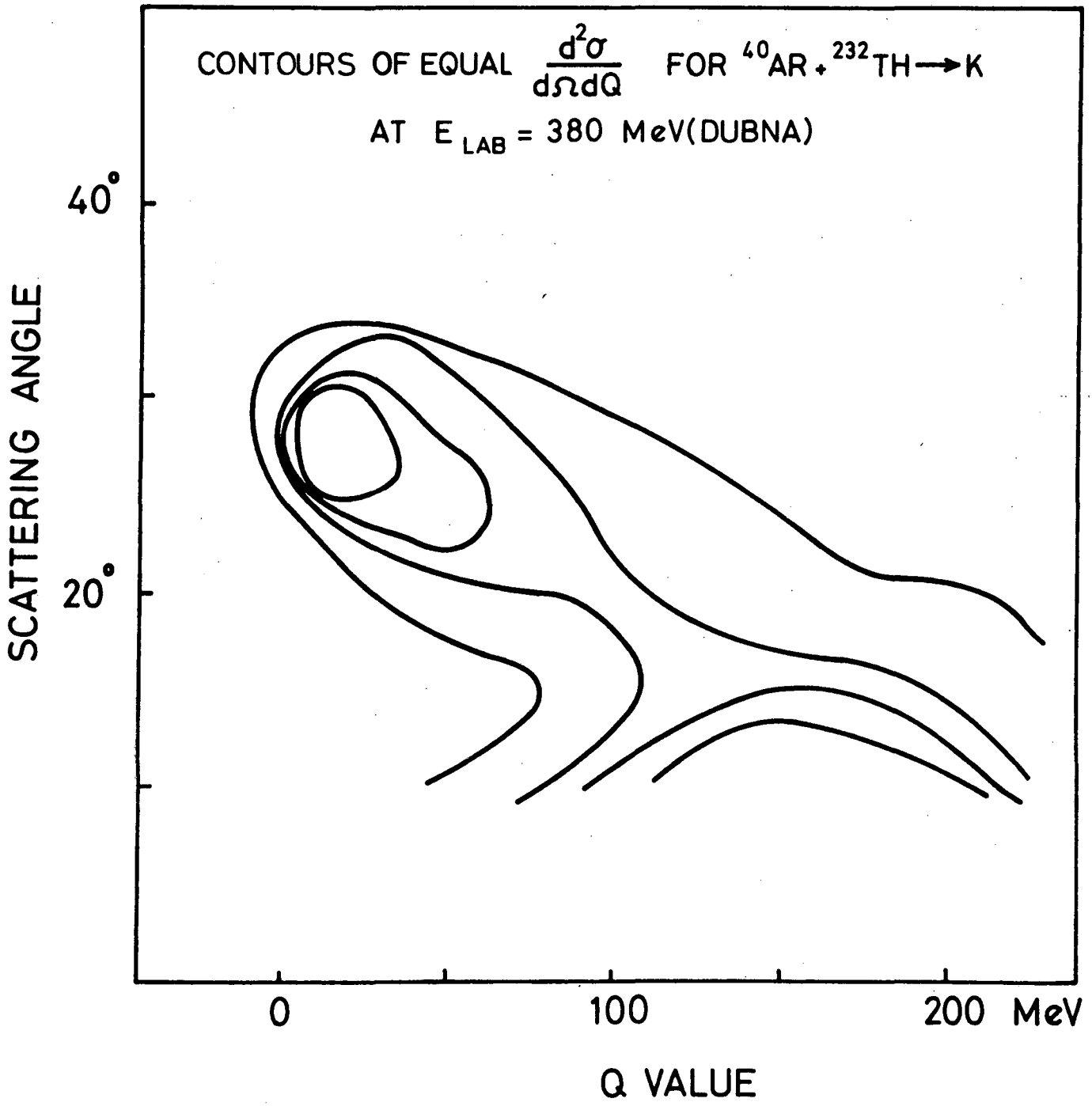
CONTOURS OF EQUAL $\frac{d^2\sigma}{d\Omega dQ}$ FOR $^{40}AR + ^{232}TH \rightarrow K$
AT E_{LAB} = 380 MeV(DUBNA)
40°
20°
SCATTERING ANGLE
0
100
200 MeV
Q VALUE

Fig. 20

TECHNICAL INFORMATION DIVISION
LAWRENCE BERKELEY LABORATORY
UNIVERSITY OF CALIFORNIA
BERKELEY, CALIFORNIA 94720